relatively large area of the atrium is involved in the circuit. In sporadic case reports, different ventriculoatrial (VA) block patterns during AVNRTs, including complete VA block,[1,2,6,7] second-degree Wenckebach-type VA block,[6–12] 2:1 VA block,[2,8,12–15] intermittent loss of atrial depolarizations,[3,9,16,17] and variable His-atrial (HA) conduction times during a fixed His-His (HH) interval with 1:1 VA relationship,[1,2,18] were interpreted as suggesting the presence of an upper common pathway between the circuit and the atrium. However, the precise mechanisms of the different VA block patterns and the effects of SP ablation on AVNRTs with different VA block patterns[6,8,11–13,16–18] have not been described in a series of patients.

The purposes of this study were to (1) characterize AVNRTs with different VA block patterns, (2) elucidate the mechanisms of different VA block patterns, and (3) assess the effects of conventional SP ablation on AVNRTs with different VA block patterns.

Methods

Patients

Among 249 consecutive patients with AVNRT who underwent electrophysiologic study and SP ablation at our institution, 6 (2.4%) patients (1 man and 5 women; age 40 ± 22 years) exhibited different VA block patterns during AVNRT and were included in this retrospective study. The different VA block patterns comprised Wenckebach-type HA block (n = 4; cases 1–4), 2:1 HA block (n = 1; case 5), and variable HA conduction times during a fixed HH interval with a 1:1 VA relationship (n = 1; case 6).

Electrophysiologic study

All patients gave written informed consents prior to the procedures. Antiarrhythmic drugs were discontinued at least five half-lives before the procedures. With patients under local anesthesia, venous access was obtained from both femoral and antecubital veins to introduce four electrode catheters. Electrode catheters were positioned at the high right atrium, coronary sinus, His-bundle region, and right ventricle, with the proximal bipole of the coronary sinus catheter positioned at the coronary sinus ostium. The electrode catheters used to record the His-bundle electrograms were octapolar (2-mm interelectrode spacing) in five patients (cases 2–6) and quadripolar (5-mm interelectrode spacing) in the other patient (case 1). The electrodes were positioned to record the most proximal His-bundle electrograms during sinus rhythm, right ventricular pacing, and AVNRT. Bipolar electrograms were filtered through a bandpass of 30 to 500 Hz, displayed on a real-time monitor at a paper speed of 100 mm/s, and stored with 2-kHz sampling frequency on magneto-optical disks (Lab System DUO, Bard Electrophysiology or EP Lab, Quinton, MA, USA). Baseline electrophysiologic evaluations and tachycardia inductions were performed during incremental pacing and extrastimulation from the right ventricular apex, high right atrium, and coronary sinus. The possible causes of narrow QRS complex tachycardias with VA block patterns other than AVNRT, such as junctional tachycardia, intrahisian reentry, and nodofascicular tachycardia using the His-Purkinje system for anterograde conduction and a nodofascicular pathway for retrograde conduction, were excluded as previously described.[17] The diagnosis of AVNRT was made based upon the classic criteria.[1]

Assessments of electrophysiologic characteristics of AVNRTs with different VA block patterns

Definitions and analyses of different VA block patterns

In this study, "VA block" during AVNRT was defined as the absence of a consistent 1:1 VA relationship with a constant HA interval during AVNRT. The different VA block patterns comprised Wenckebach-type HA block, 2:1 HA block, and variable retrograde HA conduction times during a fixed HH interval with a 1:1 VA relationship. During AVNRTs with different VA block patterns, electrophysiologic parameters, including HH and HA intervals, as well as the range (HA_{max}, HA_{min}) and the increment (ΔHA) of HA intervals, were measured. In four patients with Wenckebach-type HA block, the HH intervals straddling the beats with HA block were measured (HH_{HAB}), and the difference between those with and without HA block (ΔHH) was calculated.

Earliest retrograde atrial activation

The earliest retrograde atrial activation site was localized by mapping the right side of the interatrial septum and the coronary sinus using the ablation catheter during AVNRT and right ventricular pacing.

Evaluation of conduction times over retrograde AV nodal pathway and lower common pathway

The concept for measurement of conduction time over the lower common pathway is shown in Figure 1.[4,19] When the conduction time over the lower common pathway is defined as x (ms) and that over the retrograde limb of the reentrant circuit plus the upper common pathway as y (ms), HA interval during AVNRT with constant HA interval (HAt in milliseconds) is expressed as y − x (Figure 1A). The HA interval during right ventricular pacing at the AVNRT cycle length (CL) (HAp in milliseconds) is expressed as y + x (Figure 1B). Resolving these formulas yields x = (HAp − HAt)/2 (Figure 1C). This hypothesis is valid only when the following prerequisites[5,19] are met: (1) retrograde conduction occurs over the same AV nodal pathway with the same conduction time during AVNRT with a constant HA interval and ventricular pacing; (2) conduction time over the lower common pathway is the same during anterograde and retrograde conduction; (3) conduction time over the upper

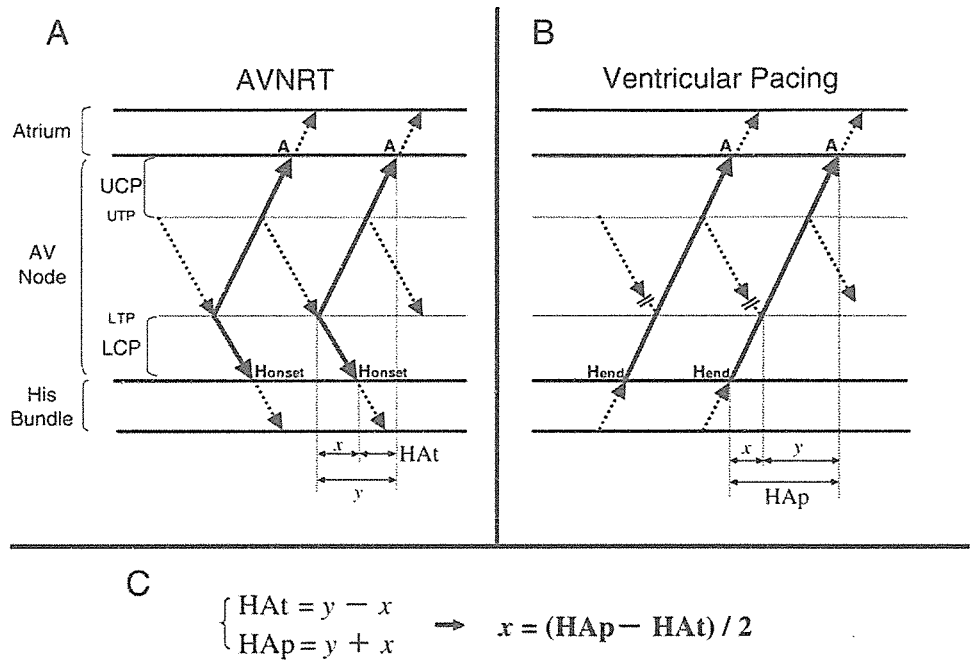

Figure 1 Concept of measurement of conduction time over the lower common pathway. Laddergrams show the activation sequences during tachycardia (**A**) and ventricular pacing at the tachycardia rate (**B**), and the formulas for calculating x (**C**). See text for details. A = earliest atrial activation; HAp = HA interval during ventricular pacing at the same rate as tachycardia; HAt = HA interval during tachycardia with stable 1:1 HA conduction; Honset and Hend = onset and end of the most proximal His-bundle electrogram, respectively; LCP = lower common pathway; LTP = lower turnaround point; UCP = upper common pathway; UTP = upper turnaround point; x = conduction time over lower common pathway; y = conduction time over the retrograde limb of the reentrant circuit and the upper common pathway.

common pathway is constant and the same during AVNRT with a constant HA interval and ventricular pacing; and (4) recording of the most proximal His-bundle potential corresponds to the proximal end of the His bundle. According to Heidbüchel et al,[19] measurements of HAp and x were helpful in differentiating the slow-slow from the slow-fast form of AVNRT, and HAp ≥70 ms (sensitivity ≥86%, specificity ≥97%) or x ≥7.5 ms (sensitivity = 100%, specificity ≥89%) was highly indicative of the slow-slow form of AVNRT. HAt was measured from the onset of the most proximal His-bundle potential to onset of the earliest atrial potential during stable AVNRT CL (CL variability <5 ms). If the atrial potential was superimposed on the ventricular potential, single ventricular extrastimuli were delivered from the right ventricle without resetting the AVNRT to dissociate the ventricular from the atrial potential and to clarify the onset of the atrial potential. When the His-bundle potential was obscured by the superimposed atrial potential during AVNRT, the timing of onset of the His-bundle potential was inferred from the HV interval during AVNRT, thereby allowing measurement of HA intervals. HAp was measured from the end of the most proximal His-bundle potential to onset of the earliest atrial potential during pacing from the right ventricular apex (n = 1) or parahisian right ventricle (without direct capture of His bundle or right bundle branch) (n = 5) at the AVNRT CL immediately after termination of the AVNRT to minimize the changes in autonomic tone.[5] When the atrial potential preceded the His-bundle potential during AVNRT (HAt <0 ms), the lower common pathway was considered to be present (x = y − HAt >0 ms).[20]

Radiofrequency catheter ablation of SP

SP ablation was performed during sinus rhythm at the classic SP region between the coronary sinus ostium and the tricuspid annulus using the electroanatomic approach.[21] Using a radiofrequency pulse generator (EPT 1000TC), 550-kHz unmodulated current was delivered between the distal tip of the 4-mm-tip ablation catheter and the indifferent patch electrode positioned on the patient's back. Current was applied in temperature-controlled mode, with an upper temperature limit of 60°C, maximal power output 40 W, and duration ≤60 seconds for each application. SP ablation was performed at the right septal region if the ablations at the right inferoparaseptal region were unsuccessful. Inducibility of AVNRT was assessed after each application. Successful ablation was defined as elimination of anterograde SP conduction or induction of only one AV nodal echo beat for at least 30 minutes after the last energy application under isoproterenol infusion.[1]

Statistical analysis

All continuous variables are expressed as mean ± SD.

Table 1 Baseline electrophysiologic characteristics

		SR			AV			VA		
Case	Types of VAB	AA	AH	HV	WCL	ERP_{FP}	ERP_{SP}	REAS	WCL	ERP
1	W	1000	80	40	362	500/300	≤500/220	S	350	≤500/230
2	W	880	112	35	370	500/270	≤500/220	S	370	500/230
3	W	920	90	35	380	500/300	≤500/240	S	360	≤500/240
4	W	830	104	42	380	500/320	500/240	S	360	≤500/240
5	(−)	920	66	46	360	600/280	≤600/220	I (1:1)	350	600/220
	2:1							S (2:1)	360	600/340
6	VHACT	800	70	45	300	600/360	600/240	S	360	600/340

Values are given in milliseconds.

AV = anterograde AV nodal conduction; ERP_{FP} = effective refractory period of fast pathway; ERP_{SP} = effective refractory period of slow pathway; I = inferoparaseptum; REAS = retrograde earliest activation site; S = superoparaseptum; SR = sinus rhythm; VA = retrograde AV nodal conduction; VAB = ventriculo-atrial block; VHACT = variable HA conduction time during fixed AVNRT cycle length; W = AVNRT with Wenckebach-type VA block; WCL = Wenckebach cycle length; 1:1 = AVNRT with 1:1 HA conduction; 2:1 = AVNRT with 2:1 HA block.

Results

Baseline electrophysiologic characteristics

Baseline electrophysiologic characteristics of the patients are given in Table 1. All six patients had normal AH and HV intervals during sinus rhythm without any ventricular preexcitation. Anterograde dual AV nodal pathway physiology was manifested as a sudden "jump-up" in AH interval during atrial extrastimulation and related to AVNRT induction at baseline state in all six patients. No patient had retrograde AV nodal dual pathway physiology. All retrograde HA conductions exhibited decremental properties and were demonstrated to be retrograde AV nodal conduction by parahisian pacing.[22] The earliest retrograde atrial activation site during right ventricular pacing was located at the right superoparaseptum at baseline in all but case 5, in whom the earliest activation shifted from the right inferoparaseptum to superoparaseptum after SP ablation.

Characteristics of AVNRTs with different VA block patterns

The characteristics of AVNRTs induced in the six patients are summarized in Table 2. In 4 patients (66%, cases 1–4), AVNRTs were associated with earliest retrograde atrial activation at the right superoparaseptum and spontaneous episodes of Wenckebach-type HA block. In 1 patient (17%, case 5), AVNRT with episodes of transient 2:1 HA block was induced after ablations at the classic SP region for the slow-slow form of AVNRT and was associated with the earliest atrial activation at the right superoparaseptum. In the remaining 1 patient (17%, case 6), AVNRT showed a 1:1 VA relationship with variable HA conduction times and multiple atrial activation sequences, whereas the HH interval was constant.

AVNRTs with Wenckebach-type HA block (cases1–4)

AVNRTs with spontaneous episodes of Wenckebach-type HA block were induced by double atrial extrastimulation, as were AVNRTs with 1:1 HA conduction (Figure 2). The atrial activation sequences were identical during both 1:1 HA conduction and Wenckebach HA block for all AVNRTs. Although HA and HH intervals both were constant during AVNRTs with 1:1 HA conduction, HA interval gradually prolonged from 85 ± 32 ms to 125 ± 43 ms (HA increment 40 ± 11 ms) just prior to HA block, and HH intervals remained constant during episodes of Wenckebach-type HA block (Table 2 and Figure 2). The HH interval reproducibly prolonged by 11 ± 3 ms for only one cycle straddling the HA block and subsequently returned to the value before HA block (Table 2 and Figure 2C). The HH interval during Wenckebach-type HA block was shorter than that during 1:1 HA conduction in three patients (cases 2–4; 328 ± 19 ms vs 389 ± 10 ms) and was almost similar in the other patient (case 1; 362 vs 364 ms). During retrograde HA conduction, mean HAp and HAt were 148 ± 61 ms and 114 ± 50 ms, respectively; therefore, mean x was calculated to be 17 ± 7 ms. HAp was >70 ms in three of four patients (case 2–4), and x was >7.5 ms in all four patients (Table 2). Therefore, AVNRTs in these four patients were estimated to have lower common pathways of considerable length. Perpetuation of AVNRT without depolarizations of the perinodal atrium, including the earliest atrial activation site (i.e., right superoparaseptum), demonstrated that the atrium is not a necessary upper link between the anterograde and retrograde limbs of the reentrant circuit. These findings are compatible with the concept of reentry within the functionally protected AV nodal area with both an upper common pathway and a lower common pathway (Figure 2).

AVNRT with 2:1 HA block (case 5)

Initially, the slow-slow form of AVNRT with consistent 1:1 HA conduction was induced by atrial extrastimulation in case 5 (Figure 3A). Earliest atrial activation during AVNRT was localized at the right inferoparaseptum, and HAt, HAp, and x were 135, 150, and 8 ms, respectively (Table 2). After the second radiofrequency energy application at the classic SP region, however, AVNRT with 2:1 HA block was reproducibly induced by atrial extrastimulation after an AH "jump-up" (Figure 3B). Earliest atrial activation shifted

Table 2 Tachycardia characteristics

Case	REAS	Type of VAB	AVNRT (1:1) HH	AH	HAt	VP PCL	HAp	x	AVNRT (W) HH	HH_{HAB}	ΔHH	HA_{min}	HA_{max}	ΔHA
1	S	W	362	318	44	360	60	8	364	376	12	38	62	24
2	S	W	400	285	115	400	150	18	315	325	10	97	145	48
3	S	W	387	230	157	390	190	17	320	327	7	110	155	45
4	S	W	380	240	140	380	190	25	350	365	15	95	138	43
Average			382 ± 16	268 ± 41	114 ± 50	383 ± 17	148 ± 61	17 ± 7	337 ± 24	348 ± 26	11 ± 3	85 ± 32	125 ± 43	40 ± 11

Case	REAS	Type of VAB	AVNRT (1:1) HH	AH	HAt	VP PCL	HAp	x	AVNRT (2:1) HH	HH_{HAB}	AH	HAt
5	I (1:1)	(−)	370	235	135	(370)*	(150)*	(8)*	—	—	—	—
	S (2:1)	2:1	—	—	—	370	222	18	370	370	183	187

Case	REAS	Type of VAB	AVNRT (1:1) HH	AH	HAt	VP PCL	HAp	x	AVNRT (VHACT) HH	AH_{min}	AH_{max}	ΔAH	HA_{min}	HA_{max}	ΔHA
6	S	VHACT	—	—	—	—	—	—	307	255	339	84	−32	52	84
Average			380 ± 15	262 ± 38	118 ± 44	380 ± 16	162 ± 63	17 ± 6	338 ± 27						

Values are given in milliseconds.

AH_{max} = maximal AH interval; AH_{min} = minimal AH interval; ΔAH = increment of AH interval; ΔHA = increment of HA interval; ΔHH = increment of HH interval at HA block; HA_{max} = maximal HA interval; HA_{min} = minimal HA interval; HH_{HAB} = HH interval straddling HA block; I = inferoparaseptum; PCL = pacing cycle length; REAS = retrograde earliest activation site; S = superoparaseptum; VAB = ventriculoatrial block; VHACT = variable HA conduction time during fixed AVNRT cycle length; VP = ventricular burst pacing; W = AVNRT with Wenckebach-type HA block; 1:1 = AVNRT with 1:1 HA conduction; 2:1 = AVNRT with 2:1 HA block.

*Not included in average values.

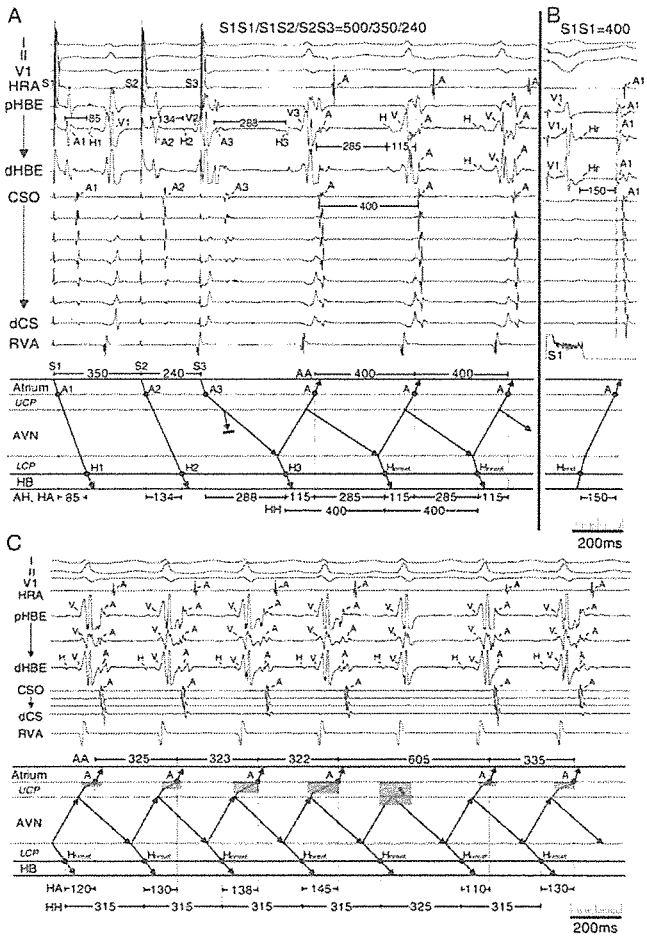

Figure 2 Body surface and intracardiac electrocardiograms during induction of atrioventricular nodal reentrant tachycardia (AVNRT) with 1:1 HA conduction by double atrial extrastimulation from the high right atrium (**A**), ventricular pacing at 400 ms from the right ventricular apex (**B**), and a spontaneous episode of Wenckebach-type HA block (**C**). Laddergrams depict the activation sequences in case 2. The *gray areas* in the laddergram indicate the postulated areas with functional conduction delay and block. See text for details. A = atrial potential; AVN = atrioventricular node; CSO = coronary sinus ostium; dCS = distal coronary sinus; HB = His bundle; Hr = retrograde His-bundle potential; HRA = high right atrium; pHBE/dHBE = proximal/distal His-bundle electrogram; RVA = right ventricular apex. Other abbreviations as in Figure 1.

from right inferoparaseptum to superoparaseptum with marked prolongation of HAt; however, AVNRT CL was unchanged. AVNRT with 2:1 HA block had HAt, HAp, and x of 187, 222, and 18 ms, respectively (Table 2) and therefore was estimated to have a lower common pathway of considerable length. AVNRT with 2:1 HA conduction presumably shared the identical reentrant circuit with AVNRT with 1:1 HA conduction (Figure 3). Perpetuation of AVNRT without depolarizations of the perinodal atrium, including the earliest atrial activation site, demonstrated that the atrium is not a necessary upper link between the anterograde and retrograde limbs of the reentrant circuit. These findings are compatible with the concept of reentry within the functionally protected AV nodal area with two atrial exits and a lower common pathway.

AVNRT with variable HA conduction times during a fixed HH interval (case 6)

AVNRT was reproducibly induced by double atrial extrastimulation after a sudden jump-up in AH interval and was associated with a 1:1 VA relationship. However, marked variations in HA (−32~52 ms) and AA intervals (236~388 ms) were observed, whereas the HH interval (307 ms) was constant (Table 2 and Figure 4). A negative HA interval during AVNRT suggested the presence of a lower common

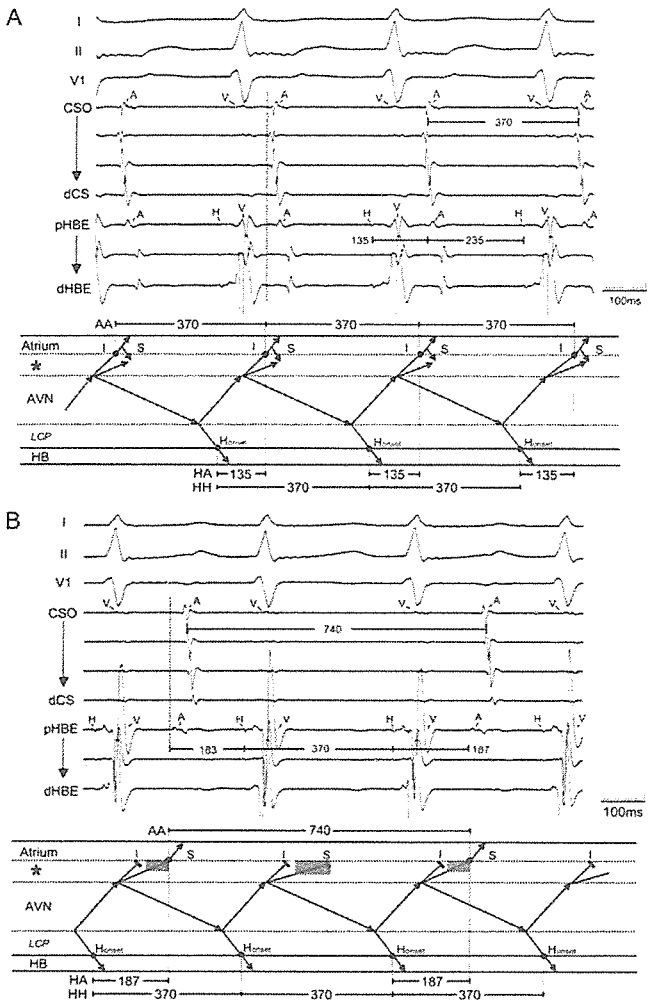

Figure 3 Body surface and intracardiac electrocardiograms during atrioventricular nodal reentrant tachycardias (AVNRTs) with 1:1 (**A**) and 2:1 HA conduction (**B**) induced at baseline and after the second radiofrequency energy application, respectively. Laddergrams depict the activation sequences in case 5. The *gray areas* in the laddergram indicate the postulated areas with functional conduction delay and block. The *vertical dotted lines* in the electrocardiograms indicate the onset of earliest atrial activation. The *asterisk* indicates a zone of tissues responsible for 2:1 HA conduction. See text for details. I = inferoparaseptal atrial exit; S = superoparaseptal atrial exit. Other abbreviations as in previous figures.

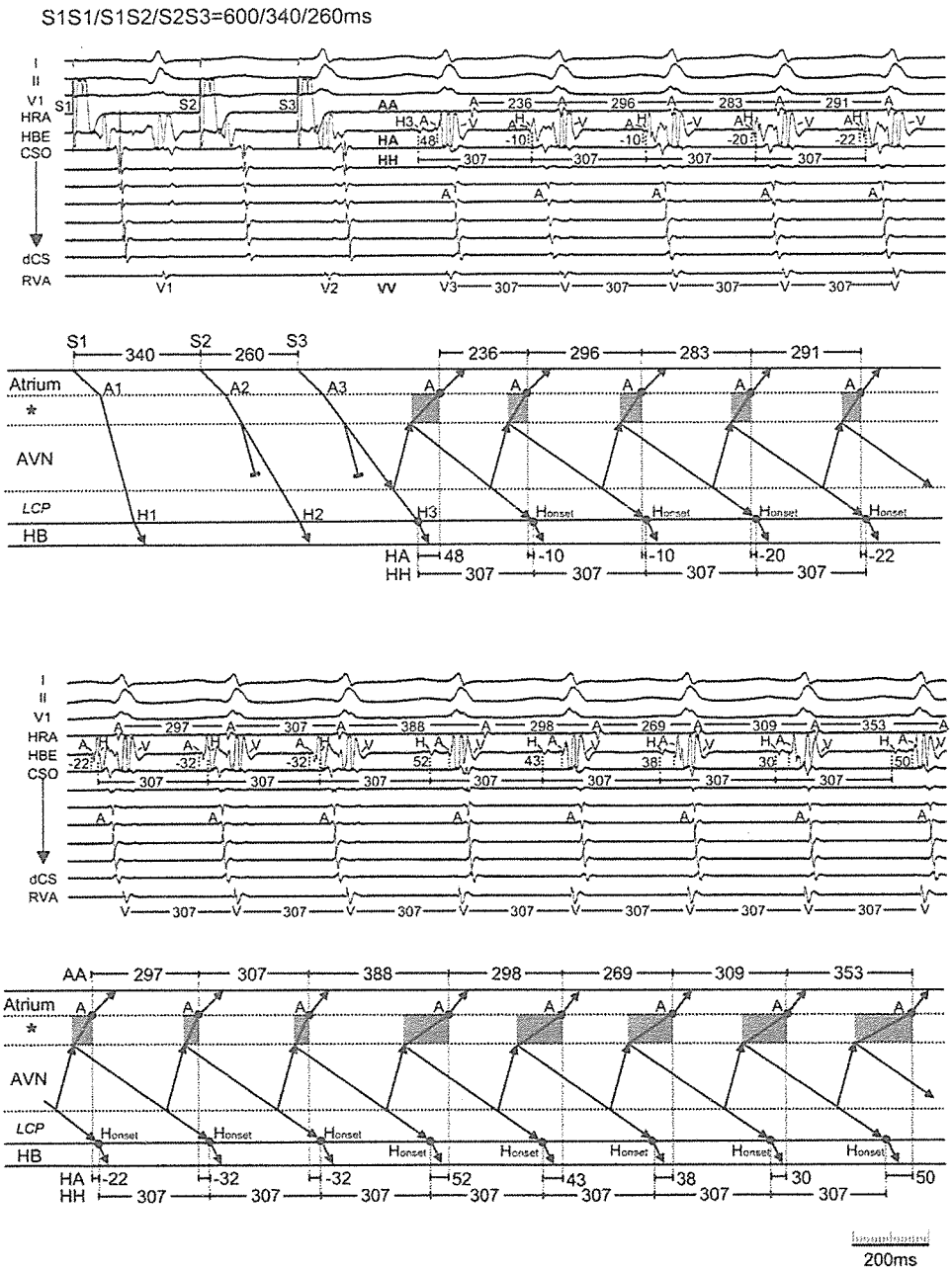

Figure 4 Body surface and intracardiac electrocardiograms during induction of atrioventricular nodal reentrant tachycardia (AVNRT) by double atrial extrastimulation (S1S1/S1S2/S2S3 = 600/340/260 ms) from the high right atrium (HRA) in case 6. Note variable AA and HA intervals with a fixed AVNRT cycle length. Multiple retrograde atrial activation sequences with changes in intra-atrial conduction times from the His-bundle region (HBE) to the high right atrium (HRA) and coronary sinus suggest multiple atrial exits from the reentrant circuit. The upper and the lower strips are continuous. The *gray areas* in the laddergram indicate the postulated areas with functional conduction delay. The *asterisk* indicates a zone of tissues responsible for variable HA conduction. See text for details. Abbreviations as in previous figures.

pathway as previously described.[20] Multiple atrial activation sequences with variable HA intervals and earliest atrial activations at the right superoparaseptum were observed (Figure 4). HAp was not available because retrograde Wenckebach CLs (360 ms) were longer than the HH interval during AVNRT (307 ms), suggesting the presence of a lower common pathway between the circuit and the His bundle.[4] The longest HA interval during 1:1 HA conduction for right ventricular pacing (at paced CL 370 ms) was 128 ms (not shown) and was much longer than any HA intervals during AVNRT (−32~52 ms). These findings are compatible with the concept of reentry within the functionally protected AV nodal area with multiple atrial exits and a lower common pathway.[9,18]

Results of SP ablation

Results of classic SP ablation are given in Table 3. After ablation with 5 ± 2 energy applications at the classic SP region, anterograde dual pathway physiology was eliminated, and AVNRT was rendered noninducible in 5 (83%) of 6 patients. In the remaining one patient (17%, case 4), nonsustained AVNRT (two to three AV nodal echo beats) remained inducible even after nine energy applications at the right inferoparaseptum and septum. In this patient, ablation modified the conduction property of the anterograde SP but not that of the retrograde AV nodal pathway. The effective refractory period and Wenckebach CL of the anterograde SP prolonged to 280 ms (basic CL 500 ms, prea-

Table 3 Results of classic slow pathway ablation

Case	REAS	Type of VAB	Rhythm	Ablation site	JT	VAB	AVB	No. RF	DPP	Acute result	Follow-up (months)	Recurrence
1	S	W	SR	I	(+)	(−)	(−)	6	(−)	Success	5	(−)
2	S	W	SR	I	(+)	(−)	(−)	3	(−)	Success	50	(−)
3	S	W	SR	I	(+)	(−)	(−)	5	(−)	Success	17	(−)
4	S	W	SR	I-MS	(+)	(−)	(−)	9	(+)	Failure	60	(−)
5	I (1:1)	(−)	SR	I	(+)	(−)	(−)	2	(−)	Success	70	(−)
	S (2:1)	2:1		I	(+)	Transient		2				
6	S	VHACT	SR	I	(+)	(−)	(−)	5	(−)	Success	70	(−)
								5 ± 2		5/6 (83%)	45 ± 28	0/6 (0%)

AVB = atrioventricular block; DPP = anterograde dual pathway physiology after ablation; I = right inferoparaseptum; JT = junctional tachycardia; MS = right midseptum; no. RF = number of radiofrequency energy applications; REAS = retrograde earliest activation site; S = right superoparaseptum; SR = sinus rhythm; VAB = ventriculoatrial block; VHACT = variable HA conduction time during fixed AVNRT cycle length; W = Wenckebach-type HA block; 1:1 = 1:1 HA conduction; 2:1 = 2:1 HA block;

blation 240 ms) and 420 ms (preablation 380 ms), respectively. The AH interval of the nonsustained AVNRT induced after SP ablation prolonged to 300 ms (preablation 240 ms), whereas the HA interval shortened to 100 ms (preablation 140 ms). Nonsustained AVNRTs were always terminated by AH block. In all patients, the accelerated junctional rhythm was induced by each energy application at the classic SP region where sharp SP potentials could be recorded.[21] No injury to the anterograde fast pathway was demonstrated after SP ablation in the six patients. In case 5, during the first energy application at the classic SP region, the accelerated junctional rhythm was associated with a short HA conduction time and a retrograde atrial activation sequence identical to that observed during ventricular pacing and AVNRT at baseline (Figure 5A). During the second to fourth energy applications at the right inferoparaseptum, the junctional rhythm was associated with a longer HA conduction time and a distinct retrograde atrial activation sequence similar to that observed during AVNRT with 2:1 HA block induced after the second energy application (Figure 5B). Four radiofrequency energy applications at the right inferoparaseptum successfully eliminated the AVNRT with 2:1 HA block. During postablation follow-up of 45 ± 28 months, no recurrence was observed among the six patients, without administration of antiarrhythmic drugs.

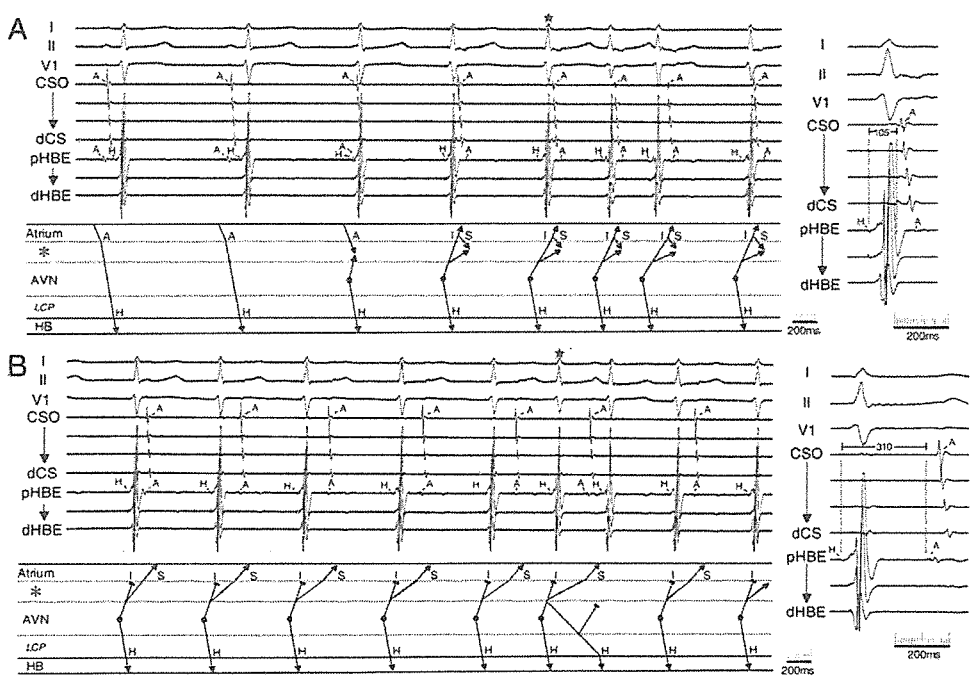

Figure 5 Body surface and intracardiac electrograms during accelerated junctional rhythms with two different retrograde atrial activation sequences induced by first (**A**) and second (**B**) application of radiofrequency energy at the classic slow pathway region. Laddergrams depict the activation sequences in case 5. Junctional beats with *stars* are shown at a faster paper speed on the *right*. The *asterisk* indicates a zone of tissues responsible for 2:1 HA conduction during atrioventricular nodal reentrant tachycardia. See text for details. Abbreviations as in previous figures.

Discussion

Mechanisms of different VA block patterns during AVNRTs

Wenckebach-type HA block

The fact that AVNRT CL was shorter during retrograde HA Wenckebach periodicity than 1:1 retrograde HA conduction in three of four patients seems to reflect a rate-dependent decremental property of the upper common pathway, which probably was composed of tissues with AV node-like electrophysiology, such as the AV node and transitional cells.[23] The consistent prolongation of the HH interval for only one cycle straddling HA block might be explained by retrograde block at the distal portion of the upper common pathway (near the upper turnaround), with some depressive influences on the circuit or a transient change in autonomic tone resulting in transient local conduction slowing at the circuit (Figure 2C). Theoretically, perpetuation of AVNRT despite HA block also might be explained by tachycardia termination at the beats with HA block and immediate reinitiation with premature junctional beats or double ventricular responses without subatrial reentry, although these possibilities seem unlikely.

2:1 HA block

The fact that the CLs were identical between AVNRTs with 1:1 and 2:1 HA conduction indicates that they shared the same subatrial reentrant circuit with different atrial exits (Figure 3). Right inferoparaseptal ablation transected the inferior (posterior) atrial exit without interrupting the circuit, allowing the superior (anterior) atrial exit to manifest (Figure 3B). These observations cannot be explained by the concept of subatrial reentry with a single upper common pathway but are consistent with the concept of subatrial reentry with multiple atrial exits and a shift of upper turnaround after inferoparaseptal ablation. This concept would be compatible with orthodromic capture of the earliest retrograde atrial activation site during entrainment of AVNRT from the atrium,[24] which frequently has been cited as evidence that the atrium forms an upper link of the circuit. It was evident that most portions of the atrium were not involved in the circuit, although the exact site of 2:1 HA block could not be localized to a small rim of perinodal atrium, AV node, or transitional cell zone[23] based solely on the observed findings. The 2:1 HA block also could be theoretically explained by double ventricular responses to retrograde atrial activations; however, the similarity of HH intervals between AVNRTs with 1:1 and 2:1 HA conduction argues against this possibility.

Variable HA conduction time during a fixed HH interval with 1:1 VA relationship

Invariable AVNRT CL despite a variable HA conduction time and retrograde atrial activation sequences (Figure 4) is consistent with the concept of intranodal reentry with multiple atrial exits[9] and is considered to result from conduction delay of various degrees over the tissues that connected the reentrant circuit to the atrium.[18] Multiple atrial activation sequences also might be explained by inhomogeneous intra-atrial conduction with a single atrial exit from an upper common pathway.

Classification of AVNRT into subforms

AVNRT is conventionally classified into slow-fast, slow-slow, or fast-slow form according to the AH interval for the anterograde limb and the site of earliest atrial activation for the retrograde limb.[5,25] Judging from inductions of AVNRT by a sudden AH jump-up and the earliest atrial activation at the right superoparaseptum, the six AVNRTs should be categorized as the slow-fast form. However, results from assessment of HAp and x suggest that the AVNRTs in this study are atypical for the slow-fast form in terms of a long HA interval during ventricular pacing at AVNRT CL (n = 5) and the presence of a lower common pathway (n = 6).[19] Therefore, they might belong to a category of a yet-unrecognized variant subform.

Effect of SP ablation

To our knowledge, only eight case reports of SP ablation for AVNRT with VA block have appeared in the literature.[6,8,11–13,16–18] In seven of these cases (88%), classic SP ablation at the right inferoparaseptum reportedly was successful.[6,11–13,16–18] In the other report (12%), SP ablation was unsuccessful, and the authors concluded the circuit might be confined within compact AV node.[8] In our study, classic SP ablation was successful in 83% of patients (n = 5), suggesting that the circuit involves not only compact AV node but also the classic SP region as a critical component. The classic SP region has been reported to contain specialized conduction tissues, such as posterior nodal extensions serving as the SP.[26,27] Participation of a small rim of perinodal atrium at the right inferoparaseptum as a critical component of the circuit cannot be definitively ruled out; however, most parts of the atrium would not be involved in the circuit. In the one patient in whom classic SP ablation was not successful (case 4), the circuit might be confined within the upper portion of the triangle of Koch. Unexpected long-term success in case 4 might be explained by a partial injury to the anterograde SP resulting in the inability to conduct in a 1:1 fashion at the tachycardia rate.

Dimension of AV node

Morphologic studies of the AV node have demonstrated a superior dense network of nodal tissue (compact AV node) and an inferior, more open portion of the AV node into which atrial bands gradually merged (transitional cell zone).[28,29] Furthermore, the studies showed that the superficial transitional fibers of AV input run along the anterior

limbus of the fossa ovalis and form the superior AV nodal input. This three-dimensional reconstruction demonstrated that AV nodal tissue occupies the bulk of the triangle of Koch. Much of the previous disagreement on the role of the atrium in the genesis of the reentrant circuit seems to derive from the definition of the extent of the AV node, especially the failure to recognize the open node as specialized tissue that is part of the AV node. In this context, it should be noted that the reentrant circuits of the AVNRTs in this study are confined to the "AV node," although participation of a small rim of perinodal atrial tissue cannot be definitively excluded. The results from experimental studies add validity to our hypothesis.[30,31]

Study limitations

This study has several technical limitations. Measurements of HAp might be inaccurate because of poor separation of the retrograde His-bundle potential from the ventricular potential. Because this was a retrospective analysis, no special effort was made to assess the role of perinodal atrium in the reentrant circuit, such as dissociating the atrium from the tachycardia by introducing an atrial extrastimulus. Therefore, the participation of a small rim of perinodal atrium as an upper link between the slow and fast pathways is not known. The postulated interpretation of the Wenckebach HA block pattern (Figure 2C) was based upon the assumption that conduction times over the lower common pathway and the reentrant circuit were constant during episodes of Wenckebach HA block. If this were not the case, the invariable HH interval during progressive HA delay would not result from the constancy of AVNRT CL but from reciprocal changes in conduction times over the lower common pathway and the reentrant circuit. Thus, such alternative explanations would be possible. The mechanisms responsible for the high prevalence (n = 6, 100%) of lower common pathways in the six AVNRT patients with VA block patterns are unclear. It was speculated that in the circuit of AVNRTs with VA block patterns, the functional conduction disturbance was present not only at the tissue connecting the atrium and the circuit but also at the lower common pathways.[11] Whether findings and interpretations of this study can be extrapolated to all patients with AVNRT is unknown.

Conclusion

AVNRTs with different VA block patterns had unique electrophysiologic characteristics, including earliest retrograde atrial activation at the right superoparaseptum (6/6 patients), longer retrograde HA conduction time (5/6 patients), and the presences of lower common pathways (6/6 patients). The different VA block patterns were considered to result from conduction delay and block at the tissues connecting the circuit to the atrium, such as AV nodal cell, transitional cell, or perinodal atrium extrinsic to the circuit. Successful ablations at the conventional SP region in most of the patients suggests that most parts of the atrium are not involved in the circuit and that the circuit might be contained within a protected region around compact AV node and posterior nodal extensions.

References

1. Josephson ME. Supraventricular tachycardias. In: Josephson ME, ed. Clinical cardiac electrophysiology: techniques and interpretations. Second edition. Philadelphia: Lea & Febiger, 1993:181–274.
2. Josephson ME, Miller JM. Atrioventricular nodal reentry: evidence supporting an intranodal location. Pacing Clin Electrophysiol 1993; 16:599–614.
3. Josephson ME, Kastor JA. Paroxysmal supraventricular tachycardia. Is the atrium a necessary link? Circulation 1976;54:430–435.
4. Miller JM, Rosenthal ME, Vassallo JA, Josephson ME. Atrioventricular nodal reentrant tachycardia: studies on upper and lower "common pathways." Circulation 1987;75:930–940.
5. Otomo K, Wang Z, Lazzara R, Jackman WM. Atrioventricular nodal reentrant tachycardia: electrophysiologic characteristics of four forms and implications for the reentrant circuit. In: Zipes DP, Jalife J, eds. Cardiac electrophysiology: from cell to bedside. Third edition. Philadelphia: WB Saunders, 2000:504–521.
6. Figa F, Chiu C, Gow RM. Unusual electrophysiological findings in atrioventricular node reentrant tachycardia. Pacing Clin Electrophysiol 1995;18:1324–1326.
7. Hamdan MH, Page RL, Scheinman MM. Diagnostic approach to narrow complex tachycardia with VA block. Pacing Clin Electrophysiol 1997;20:2984–2988.
8. Calo L, Lamberti F, Ciolli A, Santini M. Atrioventricular nodal reentrant tachycardia with ventriculoatrial block and unsuccessful ablation of the slow pathway. J Cardiovasc Electrophysiol 2002;13:705–708.
9. Ino T, Tadera T, Miyamoto S, Tanaka K, Ohno T, Nagasawa K, Hayakawa H. Ventriculoatrial block during atrioventricular nodal reentrant tachycardia utilizing multiple retrograde pathways. J Cardiovasc Electrophysiol 1998;9:1206–1213.
10. Bauernfeind RA, Wu D, Denes PO, Rosen KM. Retrograde block during dual pathway atrioventricular nodal reentrant paroxysmal tachycardia. Am J Cardiol 1978;42:499–505.
11. Kantharia BK, Mittleman RS. Case report: anterograde 2:1 and retrograde 3:2 Wenckebach block during atrioventricular nodal tachycardia: controversies of the upper and lower common pathways. J Interv Card Electrophysiol 2000;4:605–610.
12. Morady F. Ventriculoatrial block during a narrow-QRS tachycardia: what is the tachycardia mechanism? J Cardiovasc Electrophysiol 1996; 7:174–177.
13. Miles WM, Hubbard JE, Zipes DP, Klein LS. Elimination of AV nodal reentrant tachycardia with 2:1 VA block by posteroseptal ablation. J Cardiovasc Electrophysiol 1994;5:510–516.
14. Wellens JJ, Wesdorp JC, Duren D, Lie KI. Second degree block during reciprocal atrioventricular nodal reentrant tachycardia. Circulation 1976;53:595–599.
15. Portillo B, Mejias J, Leon-Portillo N, Zaman L, Myerburg RJ, Castellanos A. Entrainment of atrioventricular nodal reentrant tachycardias during overdrive pacing from high right atrium and coronary sinus. With special reference to atrioventricular dissociation and 2:1 retrograde block during tachycardias. Am J Cardiol 1984;53:1570–1576.
16. Chinushi M, Aizawa Y, Ogawa Y, Fujita S, Kusano Y, Miyajima S, Shibata A. Successful slow pathway ablation in a patient with atrioventricular nodal reentrant tachycardia having a proximal common pathway. Pacing Clin Electrophysiol 1998;21:1316–1318.
17. Hamdan MH, Kalman JM, Lesh MD, Lee RJ, Saxon LA, Dorostkar P, Scheinman MM. Narrow complex tachycardia with VA block: diagnostic and therapeutic implications. Pacing Clin Electrophysiol 1998; 21:1196–1206.

18. Guo HM, Nerheim P, Olshansky B. Irregular atrial activation during atrioventricular nodal reentrant tachycardia: evidence of an upper common pathway. J Cardiovasc Electrophysiol 2003;14:309–313.
19. Heidbüchel H, Ector H, Van de Werf F. Prospective evaluation of the length of the lower common pathway in the differential diagnosis of various forms of AV nodal reentrant tachycardia. Pacing Clin Electrophysiol 1998;21:209–216.
20. Heidbüchel H, Jackman WM. Catheter ablation of atypical atrioventricular nodal reentrant tachycardia. In: Zipes DP, Haissaguerre M, eds. Catheter ablation of arrhythmias. Second Edition. Armonk, NY: Futura Publishing Company, 2002:249–276.
21. Jackman WM, Beckman KJ, McClelland JH, Wang X, Friday KJ, Roman CA, Moulton KP, Twidale N, Hazlitt HA, Prior MI. Treatment of supraventricular tachycardia due to atrioventricular nodal reentry, by radiofrequency catheter ablation of slow-pathway conduction. N Engl J Med 1992;327:313–318.
22. Hirao K, Otomo K, Wang X, Beckman KJ, McClelland JH, Widman L, Gonzalez MD, Arruda M, Nakagawa H, Lazzara R, Jackman WM. Para-Hisian pacing. A new method for differentiating retrograde conduction over an accessory AV pathway from conduction over the AV node. Circulation 1996;94:1027–1035.
23. Mazgalev TN, Ho SY, Anderson RH. Anatomic-electrophysiological correlations concerning the pathways for atrioventricular conduction. Circulation 2001;103:2660–2667.
24. Satoh M, Miyajima S, Koyama S, Ishiguro J, Okabe M. Orthodromic capture of the atrial electrogram during transient entrainment of atrioventricular nodal reentrant tachycardia. Circulation 1993;88:2329–2336.
25. Sung RJ, Waxman HL, Saksena S, Juma Z. Sequence of retrograde atrial activation in patients with dual atrioventricular nodal pathways. Circulation 1981;64:1059–1067.
26. Inoue S, Becker AE. Posterior extensions of the human compact atrioventricular node: a neglected anatomic feature of potential clinical significance. Circulation 1998;97:188–193.
27. Inoue S, Becker AE, Riccardi R, Gaita F. Interruption of the inferior extension of the compact atrioventricular node underlies successful radio frequency ablation of atrioventricular nodal reentrant tachycardia. J Interv Card Electrophysiol 1999;3:273–277.
28. Anderson RH, Janse MJ, van Capelle FJ, Billette J, Becker AE, Durrer D. A combined morphological and electrophysiological study of the atrioventricular node of the rabbit heart. Circ Res 1974;35:909–922.
29. Janse MJ. Propagation of atrial impulse through the atrioventricular node. In: Touboul P, Waldo AL, eds. Atrial arrhythmias: current concepts and management. St. Louis: Mosby-Year Book, 1990:141–152.
30. Patterson E, Scherlag BJ. Slow:fast and slow:slow AV nodal reentry in the rabbit resulting from longitudinal dissociation within the posterior AV nodal input. J Interv Card Electrophysiol 2003;8:93–102.
31. Patterson E, Scherlag BJ. Longitudinal dissociation within the posterior AV nodal input of the rabbit: a substrate for AV nodal reentry. Circulation 1999;99:143–155.

"Left-Variant" Atypical Atrioventricular Nodal Reentrant Tachycardia: Electrophysiological Characteristics and Effect of Slow Pathway Ablation within Coronary Sinus

KIYOSHI OTOMO, M.D., HIDEO OKAMURA, M.D., TAKASHI NODA, M.D., KAZUHIRO SATOMI, M.D., WATARU SHIMIZU, M.D., PH.D., KAZUHIRO SUYAMA, M.D., PH.D., TAKASHI KURITA, M.D., PH.D., NAOHIKO AIHARA, M.D., and SHIRO KAMAKURA, M.D., PH.D.

From the Division of Cardiology, National Cardiovascular Center, Suita, Japan

Ablation within CS for Left-Variant Atypical AVNRT. *Introduction:* Recent anatomical and electrophysiological studies have demonstrated the presence of leftward posterior nodal extension (LPNE); however, its role in the genesis of atrioventricular nodal reentrant tachycardia (AVNRT) is poorly understood. This study was performed to characterize successful slow pathway (SP) ablation site and to elucidate the role of LPNE in genesis of atypical AVNRT with eccentric activation patterns within the coronary sinus (CS).

Methods and Results: Among 45 patients with atypical AVNRT (slow-slow/fast-slow/both = 20/22/3 patients) with concentric (n = 37, 82%) or eccentric CS activation (n = 8, 18%), successful ablation site was evaluated. Among 35/37 patients (95%) with concentric CS activation, ablation at the conventional SP region outside CS eliminated both retrograde SP conduction and AVNRT inducibility. Among eight patients with eccentric CS activation, the earliest retrograde atrial activation was found at proximal CS 16 ± 4 mm distal to the ostium during AVNRT. The earliest retrograde activation site was located at inferior to inferoseptal mitral annulus, consistent with the presumed location of LPNE. Ablation at the conventional SP region with electroanatomical approach only rendered AVNRT nonsustained without elimination of retrograde SP conduction in seven of eight patients (88%). Ablation targeted to the earliest retrograde atrial activation site within proximal CS (15 ± 4 mm distal to the ostium); however, eliminated retrograde SP conduction and rendered AVNRT noninducible in six of eight patients (75%).

Conclusion: In 75% of "left-variant" atypical AVNRT, ablation within proximal CS was required to eliminate eccentric retrograde SP conduction and render AVNRT noninducible, suggesting LPNE formed retrograde limb of reentrant circuit. *(J Cardiovasc Electrophysiol, Vol. 17, pp. 1177-1183, November 2006)*

atrioventricular nodal reentrant tachycardia, eccentric activation, leftward posterior nodal extension, catheter ablation, slow pathway

Introduction

Tawara was the first to describe the atrioventricular (AV) node and its posterior extensions that merge into the atrial myocardium.[1] Subsequent anatomical studies[2,3] have rediscovered the existence of the posterior nodal extensions (PNEs) of the compact AV node, which extended to the right inferoseptal area between the tricuspid annulus (TA) and the coronary sinus (CS) ostium on the right side and to the left inferoseptal area along the mitral annulus (MA) on the left side. The rightward PNE is thought to underlie conduction over the slow pathway (SP) during AV nodal reentrant tachycardia (AVNRT)[4-6]; however, the role of the leftward PNE in the genesis of AVNRT still remains to be elucidated. While a vast majority of AVNRTs are amenable to the right-sided SP ablation at the right inferoseptal area,[7] rare cases of both typical (slow-fast)[7-12] and atypical (slow-slow and fast-slow) forms of AVNRTs[12-15] are resistant to the standard right-sided ablation and require the left-sided ablation at the MA or within the proximal CS. Although the "left-variant" atypical AVNRT with eccentric retrograde CS activation is reported,[13-19] whether the leftward PNE participates in the formation of the reentrant circuit and the left-sided ablation is, therefore, required to eliminate such variants is controversial.

The purposes of this study were to assess (1) the incidence of atypical AVNRTs with the eccentric CS activation, (2) the effect and the efficacy of the SP ablation at the earliest retrograde atrial activation site within the CS, and (3) to reveal the possible role of the leftward PNE in the genesis of the reentrant circuit in atypical AVNRTs with the eccentric CS activation.

Address for correspondence: Kiyoshi Otomo, M.D., Department of Cardiovascular Medicine, Cardiovascular Center, Tsuchiura Kyodo Hospital, 11-7 Manabe-shin-machi, Tsuchiura, Ibaraki prefecture, 300-0053, Japan. Fax: 81-29-823-1160; E-mail: k-otomo@fj8.so-net.ne.jp

Manuscript received 9 May 2006; Revised manuscript received 30 June 2006; Accepted for publication 11 July 2006.

doi: 10.1111/j.1540-8167.2006.00598.x

Methods

Patients

Forty-five patients with atypical AVNRT (age: 30 ± 15 years, male/female: 22/23 patients) who underwent the electrophysiological study and the SP ablation were included in

TABLE 1
Patient and Electrophysiological Characteristics

	Concentric CS Activation Pattern (37 pts, 82%)	Eccentric CS Activation Pattern (8 pts, 18%)	P value
Female	18 pts (49%)	5 pts (63%)	NS
Age (years)	35 ± 15	41 ± 16	NS
Baseline			
SCL (msec)	889 ± 133	894 ± 132	NS
AH (msec)	92 ± 19	91 ± 19	NS
HV (msec)	42 ± 6	42 ± 5	NS
AV Conduction			
WCL (msec)	343 ± 25	332 ± 28	NS
ERP (msec)	252 ± 24	250 ± 23	NS
aAVNMPP	37 pts (100%)	8 pts (100%)	NS
VA Conduction			
WCL (msec)	395 ± 38	405 ± 63	NS
ERP (msec)	269 ± 31	249 ± 22	NS
rAVNDPP	24 pts (65%)	3 pts (38%)	NS
AVNRT Induction			
Isoproterenol Requirement	28 pts (76%)	6 pts (75%)	NS
Subforms of AVNRT			
Slow-slow	15 pts (41%)	5 pts (63%)	NS
Fast-slow	19 pts (51%)	3 pts (37%)	NS
Slow-slow and Fast-slow	3 pts (8%)	0 pts (0%)	NS
Slow-fast	17 pts (46%)	2 pts (25%)	NS
Slow-Slow	n = 18	n = 5	
TCL (msec)	387 ± 16	378 ± 17	NS
AH (msec)	279 ± 34	268 ± 18	NS
HA (msec)	108 ± 34	110 ± 21	NS
Fast-Slow	n = 22	n = 3	
TCL (msec)	342 ± 49	338±42	NS
AH (msec)	115 ± 23	106 ± 13	NS
HA (msec)	227 ± 61	232 ± 30	NS
Slow-Fast	n = 17	n = 2	
TCL (msec)	385 ± 24	390 ± 14	NS
AH (msec)	342 ± 34	353 ± 11	NS
HA (msec)	37 ± 11	38 ± 4	NS

aAVNMPP = anterograde atrioventricular nodal multiple pathway physiology; AH = atrial-His interval AV = atrio ventricular; AVNRT = atrioventricular nodal reentrant tachycardia; AV = atrio ventricular; CS = coronary sinus; ERP = effective refractory period; HA = His-atrium interval; HV = His-ventricle interval; NS = not significant; pt(s) = patient(s); rAVNDPP = retrograde atrioventricular nodal dual pathway physiology; SCL = sinus cycle length; TCL = tachycardia cycle length; VA = ventricular atrial; WCL = Wenckbach cycle length.

this retrospective study. Slow-slow, fast-slow, and both forms were induced in 20 (44%), 22 (49%) and 3 patients (7%), respectively, and typical (slow-fast form) AVNRT was also inducible in 19 patients (42%) (Table 1). These 45 patients with atypical AVNRT accounted for 18% of all 249 patients who underwent the electrophysiological study and the SP ablation for typical and/or atypical AVNRTs. No patient had organic heart disease.

Electrophysiological Study

All patients gave written informed consent prior to the procedures. Antiarrhythmic drugs had been discontinued for at least five half-lives before the procedures. With patients under local anesthesia, venous access was obtained from both the femoral and the antecubital veins to introduce four electrode catheters. Three quadripolar catheters were introduced from femoral veins and positioned at the high right atrium (RA), the His-bundle region and the apex of the right ventricle (RV). An octapolar catheter (2-2-2 interelectrode spacings) was introduced from the right antecubital vein and positioned within the CS. The proximal bipole of the CS catheter was located at the ostium of the CS and its position was confirmed by CS venography in all patients. Baseline electrophysiological evaluations and tachycardia inductions were performed during incremental pacing and extrastimulation (basic cycle length [CL]: 500–700 msec) from the RV apex, the high RA, and the CS. If AVNRT was not induced at baseline, isoproterenol (0.5–2.0 μg/minute) was administered intravenously to facilitate induction of tachycardia. Retrograde atrial activation sequence during atypical AVNRT was determined by the intracardiac electrograms recorded from the high RA, the His-bundle region and the CS, and the retrograde earliest atrial activation site was confirmed by mapping the right side of the interatrial septum and the CS using the ablation catheter during atypical AVNRT. Bipolar electrograms were filtered through a bandpass of 30 to 500 Hz, displayed on a real-time monitor at a paper speed of 100 mm/second and stored with 2-kHz sampling frequency on magneto-optical disks (Bard LabSystem Duo, Bard Electrophysiology, Lowell, MA, USA; or EP Lab, Quinton, Electrophysiology, Richmond Hill, Ontario, Canada). Correct electric connections of the individual CS electrodes to the recording system were confirmed by proximal-to-distal atrial activation sequence recorded from the CS during sinus rhythm.

The exclusion of tachycardia mechanisms other than AVNRT and the diagnosis of AVNRT were made based upon the classical criteria.[20] The absence of accessory pathway was confirmed by the following criteria: (1) ventricular preexcitation was absent during sinus rhythm and atrial pacing, (2) ventriculo-atrial (VA) interval during tachycardia was not lengthened by occurrence of bundle branch blocks, (3) the tachycardia was not reset by a ventricular extrastimulus delivered during His-bundle's refractoriness, and (4) "para-Hisian pacing"[21] during sinus rhythm showed retrograde AV nodal conduction pattern. Atrial tachycardia was excluded by the following criteria: (1) "V-A-V sequence" (not "V-A-A-V sequence") was observed upon cessation of ventricular pacing associated with 1:1 VA conduction during tachycardia[22] and (2) the tachycardia was reproducibly terminated with ventricular premature extrastimuli not reaching the atrium. The diagnosis of AVNRT was made if the presence of an accessory pathway and the atrial tachycardia was excluded by the criteria mentioned above.

Induced AVNRTs were classified into slow-slow, fast-slow, and slow-fast forms according to the previously described criteria.[15,23] *Slow-fast form* was diagnosed when the anterograde conduction occurred over the SP with the atrial-His (A-H) interval during tachycardia of ≥200 msec and the retrograde conduction proceeded over the fast pathway (FP) with the earliest atrial activation at the right superoseptum. *Fast-slow form* was diagnosed when anterograde conduction occurred over the FP with the A-H interval during tachycardia of <200 msec, the retrograde conduction proceeded over the SP with the earliest atrial activation at the right inferoseptum or the proximal CS and the A-H interval was shorter than the His-atrial (H-A) interval. *Slow-slow form* was diagnosed when the anterograde conduction occurred over the SP with the A-H interval during tachycardia of ≥200 msec, the retrograde conduction proceeded over the SP with the earliest atrial activation at the inferoseptum or the proximal CS and the A-H interval was longer than the H-A interval.

Classification of Retrograde Atrial Activation Sequence

According to the earliest retrograde atrial activation site, the retrograde atrial activation sequences during atypical AVNRTs were classified into two patterns: (1) the concentric CS activation pattern, in which the earliest activation was recorded at the right inferoseptum outside the CS and (2) the eccentric CS activation pattern, in which the earliest activation was recorded within the CS distal to the ostium.

SP Ablation

Irrespective of the retrograde atrial activation patterns: the SP ablation was first performed at the conventional SP region at the right inferoseptal area between the TA and the CS ostium during sinus rhythm targeting the SP potential[7] or during the retrograde SP conduction for atypical AVNRT or ventricular pacing targeting the atrial insertion of the retrograde SP where the earliest atrial activation was recorded.[7] Among those with the eccentric CS activation pattern, when the standard right inferoseptal ablation failed, the earliest atrial activation site within the CS was secondly targeted. Using the radiofrequency pulse generator (EPT 1000TC, EP Technology, Sunnyvale, CA, USA), 550-kHz unmodulated current was delivered between the distal tip of the 4-mm-tipped ablation catheter and the indifferent patch electrode positioned at the back of the patient in the temperature-controlled mode with the upper temperature limit of 60°C the maximal power output of 40 W and the duration of 60 seconds or less for each application. Inducibility of AVNRT was assessed after each application. Successful ablation was defined as elimination of the retrograde SP conduction for at least 30 minutes after the last energy application under isoproterenol infusion.[7] The effects of the ablation on the retrograde SP conduction were assessed by programmed ventricular stimulation after the SP ablation.

Statistical Analysis

All the continuous variables were expressed as mean ± SD. Two-tailed Wilcoxon *t*-test and Mann-Whitney *U* test were used to compare paired and unpaired variables between the patient groups, respectively. Yates 2×2 chi-square test or Fisher's test was used to compare the categorical variables between the patient groups. A P value of less than 0.05 was considered statistically significant.

Results

The patient characteristics are summarized in Table 1. Among 45 patients with atypical AVNRTs, the retrograde atrial activation sequences during atypical AVNRTs showed the concentric CS activation pattern in 37 patients (82%) and the eccentric CS activation pattern in the remaining 8 patients (18%). Among the 37 patients with the concentric CS activation pattern, slow-slow form was induced in 15 patients (41%), fast-slow form in 19 (51%), and both forms in 3 patients (8%). Among eight patients with the eccentric CS activation pattern, slow-slow form was induced in five (63%) and fast-slow form in three patients (37%). Typical (slow-fast form) AVNRT was also induced in 19 patients (42%). The age, the gender, proportions of each AVNRT subform, and the incidence of concomitant slow-fast form were not significantly different between the groups with the concentric and the eccentric CS activation patterns (Table 1).

Basic Electrophysiological Characteristics (Table 1)

The basic electrophysiological characteristics are summarized in Table 1. No patients had ventricular preexcitation and all had normal A-H and H-V intervals during sinus rhythm at baseline status. All patients showed anterograde multiple AV nodal pathway physiology during baseline status, including dual (n = 40, 89%), triple (n = 4, 9%) and quadruple pathway physiology (n = 1, 2%), defined by single, double and triple jump-up's in A-H interval (>50 msec) after 10-msec decrements in coupling intervals of extrastimuli during atrial extrastimulation, respectively. Retrograde dual AV nodal pathway physiology was demonstrated by a sudden jump-up in H-A (VA) interval and a simultaneous shift of the earliest retrograde atrial activation site from the superoseptal to the inferoseptal area during ventricular extrastimulation at baseline status in 19 (42%) and only after isoproterenol infusion in eight patients (18%). The remaining 18 patients (40%) had single retrograde AV nodal pathway over the SP. Retrograde 1:1 SP conduction was demonstrable during constant ventricular pacing at baseline status in 40 patients (89%) and only after isoproterenol infusion in the remaining five patients (11%). All VA conductions showed decremental property during decremental RV pacing and/or premature RV stimulation and were demonstrated to be retrograde AV nodal conduction by the para-Hisian pacing[21] in all patients. The earliest atrial activation site during the retrograde SP conduction was found at the right inferoseptal area outside the CS in 37 patients (82%) and the proximal CS in the remaining 8 patients (18%). There was no statistically significant difference in each basic electrophysiological parameter between those with the concentric and the eccentric CS activation patterns.

Characteristics of Atypical AVNRT

The characteristics of 19 typical and 48 atypical AVNRTs are summarized in Table 1. Sustained atypical AVNRT was induced at baseline status in 11 (24%) and only after isoproterenol infusion in 34 patients (76%). The earliest retrograde atrial activation site during atypical AVNRT was identical to that during retrograde SP conduction for ventricular pacing in all patients. The earliest retrograde atrial activation was recorded at the right inferoseptum outside the CS among those with the concentric CS activation pattern (n = 37), while among those with the eccentric CS activation pattern (n = 8) it was recorded at the proximal CS (16 ± 4 mm distal to the ostium) close to the inferoseptal to the inferior aspect of the MA (Figs. 1-3). The retrograde atrial activation sequence was generally fixed throughout the episodes of AVNRT with the concentric and the eccentric CS activation patterns. There was no difference in proportions of each subform, AVNRT-CL and A-H and H-A intervals of each subform between those with the concentric and the eccentric CS activation patterns (Table 1).

SP Ablation

Patients with the concentric CS activation

Among 37 patients with the concentric CS activation, the SP ablation was performed at the right inferoseptal region outside the CS during sinus rhythm (n = 6; 16%) or during retrograde SP conduction for RV pacing (n = 18, 49%) or AVNRT (n = 13, 35%), targeting the earliest atrial activation

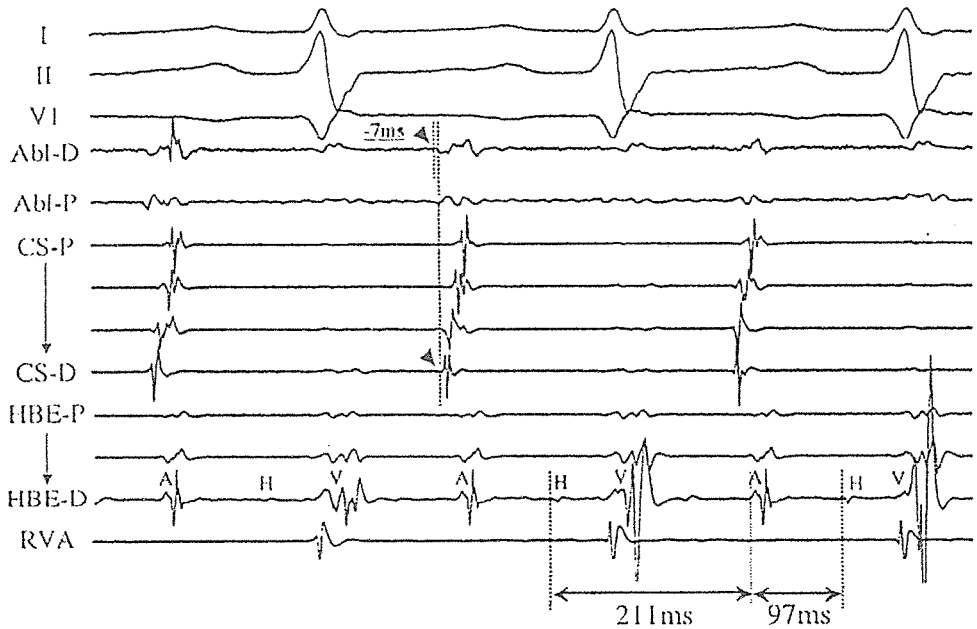

Figure 1. *Body-surface and intracardiac electrocardiograms during fast-slow form AVNRT (AH interval = 211 msec, HA interval = 97 msec) with eccentric CS activation pattern in patient 5. Atrial electrograms recorded from the ablation catheter (Abl-D and P) located at the proximal CS preceded that recorded from the distal bipole of the CS catheter (CS-D) by 7 msec, showing the eccentric CS activation pattern. See the text for details. A = atrial electrogram; CS-P and -D = proximal and distal bipole of CS catheter; H = His-bundle potential; HBE-P and -D = proximal and distal bipole of His-bundle catheter; RVA = right ventricular apex; S = stimulus; and V = ventricular electrogram. See the text for details.*

site of the retrograde SP (Table 2). Among all six patients with the SP ablation during sinus rhythm, the accelerated junctional rhythm was induced during the energy applications and the retrograde SP conduction was eliminated after the SP ablation. Among the other 31 patients with the SP ablation during the retrograde SP conduction, the retrograde SP conduction was eliminated in 29 patients, while the retrograde SP conduction was still present after the energy application in the other two patients. Thus, the retrograde SP conduction was eliminated in 35 of 37 patients (95%) with the concentric CS activation pattern after 5 ± 2 times of the energy applications at the right inferoseptum, while it was not eliminated in the other two patients (5%). The successful ablation site was located at the level of lower (n = 7, 20%), middle (n = 11,

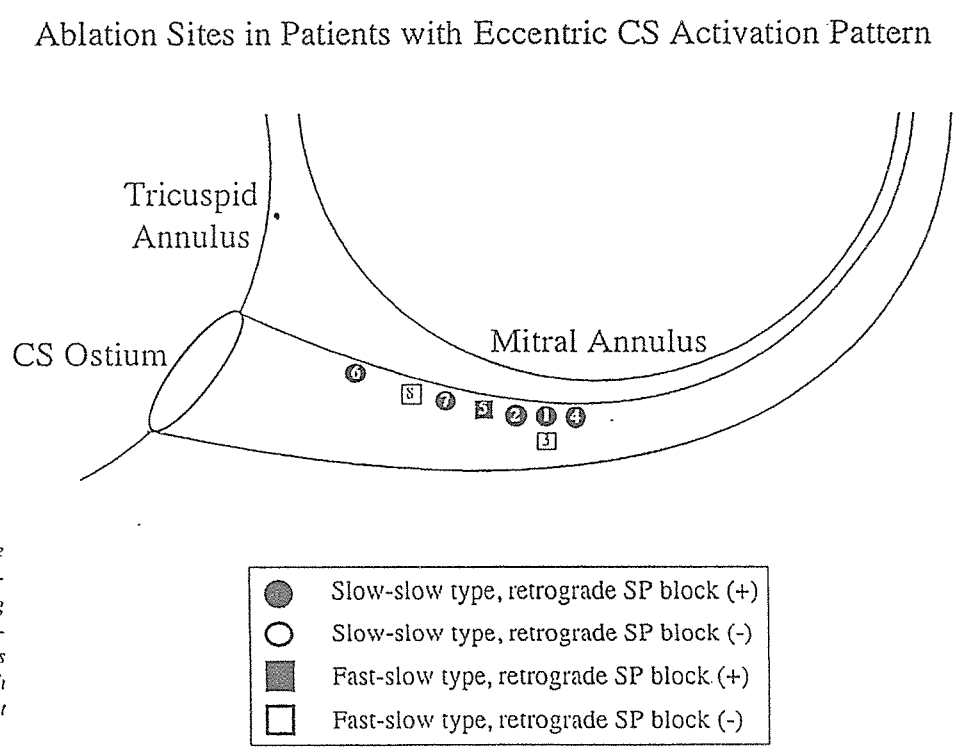

Figure 2. *Schematic representation of the sites with successful (n = 6) and unsuccessful SP ablation (n = 2) within the CS among patients with the eccentric CS activation pattern. The numbers in the circles and squares indicate the patient number among those with eccentric CS activation pattern. See the text for details. SP = slow pathway.*

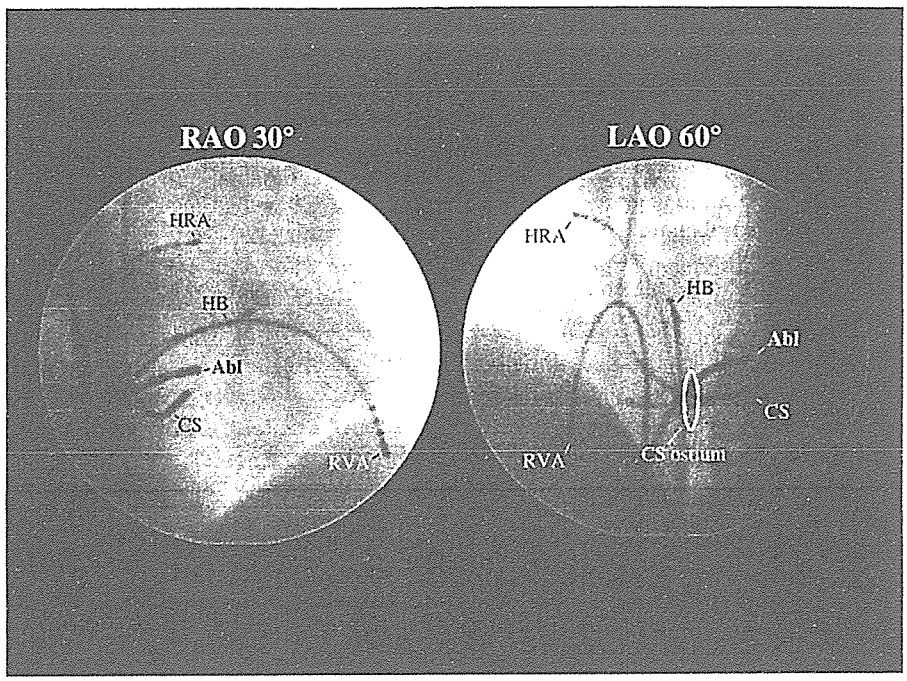

Figure 3. *Fluoroscopic views of the successful ablation site in a patient with fast-slow AVNRT with the eccentric CS activation pattern (Patient 5). The ablation catheter is located within the CS 15-mm distal to the ostium. See the text for details. Abl = ablation catheter; HB = His-bundle catheter; HRA = high right atrium; LAO = left anterior oblique view; RAO = right anterior oblique view; and RVA = right ventricular apex.*

31%) and upper one-third of the CS ostium (n = 9, 26%), the right midseptal area (n = 3, 9%) and just above the upper lip of the CS ostium (n = 5, 14%). In two patients with residual retrograde SP conduction, sustained AVNRT (n = 1) or two atypical AV nodal echo beats (n = 1) were inducible even after 10 times of energy applications at right inferoseptal and midseptal area, although the VA Wenckebach CL in these two patients slightly prolonged after ablation (before vs after ablation: 420 vs 450 msec and 380 vs 400 msec). There was no complication related to the SP ablation.

Patients with eccentric CS activation

Among eight patients with the eccentric CS activation, the SP ablation was first performed at the right inferoseptal region during sinus rhythm (Table 2). In all eight patients, accelerated junctional rhythm was induced during energy applications. After the mean of 16 ± 3 times of the energy application at the right inferoseptum and midseptum, atypical AVNRT was rendered noninducible with inducible atypical AV nodal echo beats (2 and 5 AV nodal echo beats in 6 and 1 patients, respectively) in seven patients (88%), while in the other patient (12%) sustained AVNRT was still inducible. The mean Wenckebach CL of the retrograde SP significantly prolonged after the right inferoseptal ablation (before vs after ablation: 405 ± 63 msec vs 466 ± 37 msec; P = 0.012), although the retrograde SP conduction was not eliminated in any patients. All eight patients thereafter received the SP ablation targeting the earliest atrial activation site of the retrograde SP conduction within the CS. The SP ablation was performed at the roof of the proximal CS, mean of 15 ± 4 mm (range: 7–19 mm) distal to the ostium during sinus rhythm (n = 5) or ventricular pacing with 1:1 retrograde SP conduction (n = 3) (Figs. 1-3). Among five patients with the SP ablation during sinus rhythm, accelerated junctional rhythm was induced and associated with 1:1 VA conduction over the retrograde FP (n = 2), as manifested by the earliest retrograde atrial activation registered at the right superoseptum, or over the retrograde SP (n = 3), as manifested by the earliest retrograde atrial activation registered at the proximal CS. In the latter three patients, junctional rhythm was subsequently associated with complete VA block. Among three patients with the SP ablation for the retrograde SP conduction during RV pacing, VA block was observed during the energy delivery in all three patients. After 3 ± 2 times of the energy applications, the retrograde SP conduction was eliminated in 6/8 patients (75%). In the remaining two patients with residual retrograde SP conduction, sustained AVNRT was no longer inducible but 2 and 5 AV nodal echo beats were still inducible in each patient even after six times of energy applications to the earliest retrograde activation site within the CS. In these two patients, the Wenckebach CL of the retrograde SP prolonged after the ablation at the retrograde earliest activation site within the CS (pre vs postablation: 500 vs 550 msec and 500 and 600 msec), although the retrograde SP conduction was not eliminated. There was no complication related to the SP ablation.

TABLE 2
Results of SP Ablation at Right Inferoseptal Region

	Concentric CS Activation Pattern (37 pts)	Eccentric CS Activation Pattern (8 pts)
Ablation target		
SP potential during sinus rhythm	6 pts (16%)	8 pts (100%)
Earliest atrial activation site during retrograde SP conduction	31 pts (84%)	0 pt (0%)
RF energy application number	5 ± 2*	16 ± 3*
Ablation outcome		
Inducible sustained AVNRT	1 pt (3%)	1 pt (12%)
Inducible nonsustained AVNRT	1 pt (3%)	7 pts (88%)
Retrograde SP block	35 pts (94%)	0 pt (0%)

*P < 0.01 by unpaired Student's *t*-test. AVNRT = atrioventricular nodal reentrant tachycardia; CS = coronary sinus; pt(s) = patient(s); RF = radiofrequency; SP = slow pathway.

Post-Ablation Follow-Up

No recurrence of AVNRT was observed during a mean ambulatory follow-up period of 16 ± 12 months in all 45 patients, including four patients with unsuccessful SP ablation (two with concentric and two with eccentric CS activation pattern) in whom daily oral doses of verapamil (120–240 mg/day) was temporarily continued for 1–2 months after the unsuccessful ablation and was successfully discontinued without subsequent clinical recurrences of all forms of AVNRT.

Discussion

Major Findings

The eccentric CS activation pattern was observed in 18% of patients with atypical AVNRT. The conventional right inferoseptal SP ablation did not abolish eccentric retrograde SP conduction but rendered AVNRT nonsustained. The SP ablation at the earliest retrograde activation site inside the CS (15 ± 4 mm from the ostium) eliminated the retrograde SP conduction and the AVNRT inducibility in 75%, suggesting these retrograde SPs had left-sided breakthroughs and constituted the retrograde limbs of the reentrant circuits.

Incidence of Eccentric CS Activation Pattern in AVNRT

Hwang et al.[16] reported that the earliest retrograde atrial activation was recorded within the CS in 0% (0/310 patients) among typical form and in 43% (20/46 patients) among atypical form, while Nam et al.[12] reported its incidence of 6% (3/52 patients) among typical form and 80% (8/10 patients) among atypical form. Chen et al.[18] reported its incidence of 8% (16/211 patients) among typical form and 14% (2/14 patients) among atypical form. In this study, its incidence was 18% (8/45 patients) among atypical form. The inconsistent incidence of the eccentric CS activation pattern during atypical AVNRT in different studies might be explained by relatively small number of patients included in the study population and possibly by different position of the CS catheter during the electrophysiological study in each study. Previous reports showed the higher incidence of the eccentric CS activation pattern among those with atypical (14–80%) than those with typical form (0–8%).[12,16,18] This finding suggests, regardless of whether or not the leftward PNE is the crucial part of the reentrant circuit, its retrograde activation is more frequently associated with atypical than typical form of AVNRT.

SP Ablation for Atypical AVNRT with Eccentric CS Activation

Whether the retrograde left-sided atrionodal connection constitutes the critical component of the reentrant circuit or only an innocent bystander in atypical AVNRT with the eccentric CS activation pattern is controversial.[12–19] Furthermore, whether the eccentric CS activation pattern during atypical AVNRT is the hallmark of AVNRTs that require left-sided ablation remains to be elucidated. Jackman et al.[14,15] reported that the leftward PNE constituted the retrograde limb of the reentrant circuit and the SP ablation at the earliest retrograde activation site within the proximal CS was, therefore, required to eliminate atypical AVNRT with the eccentric CS activation pattern. Nam et al.[12] demonstrated that in nine patients with atypical form of AVNRT associated with the eccentric CS activation pattern, the proximal CS was a part of reentrant circuit by entrainment pacing at the earliest retrograde activation site within the CS and that the ablation targeted to the left-sided atrionodal connection was required in two of nine patients (22%). Conversely, others postulated that the retrograde left-sided atrionodal connection was an innocent bystander; therefore, conventional right-sided SP ablation was sufficient to eliminate inducibility of atypical AVNRTs with the eccentric CS activation pattern.[16–19] Among eight patients with the eccentric CS activation in our study, the standard right-sided ablation lengthened the VA Wenckebach CL and rendered atypical AVNRT nonsustained in seven of eight patients (88%), possibly suggesting partial injury to the retrograde eccentric SP induced by the right-sided ablation. The fact that the retrograde eccentric SP conduction was eliminated only after the SP ablation at the earliest atrial activation site within the CS in addition to the standard right-sided ablation in six of eight patients (75%) would suggest that these SPs had broad atrial connection spanning between the right and left inferoseptal area, otherwise, they had a discrete left-sided atrial input and the right-sided ablation partially injured the left-sided SP only by the transseptal heating. In either case, we hypothesize these left-sided SP indeed constituted the retrograde limb of the reentrant circuit in atypical AVNRT with the eccentric CS activation. The success rate (0%) of the right-sided SP ablation for atypical AVNRTs with the eccentric CS activation pattern in our study was much lower than that in previous studies (75–100%),[12,16,18] although the maximal energy output (40 W) during the SP ablation in this study was higher than that in previous reports (Nam et al.[12]: 30 W, Hwang et al.[16]: 25 W). These inconsistent results between the reports might be explained by the different success criteria utilized in the different studies. The success criteria utilized in this study (retrograde SP block) was more rigorous than that utilized in previous studies,[12,16,18] (noninducibility criteria), which would have led to an apparently lower success rate in this study. In previous studies,[12,16,18] retrograde SP block was not achieved by the standard right-sided SP ablation in most patients while the atypical AVNRTs were rendered noninducible. In our study, "the noninducibility criteria" was achieved by the right-sided ablation in seven of eight patients (88%) with the eccentric CS activation pattern. Further studies would be required to define an optimal endpoint for the SP ablation in atypical AVNRT with eccentric CS activation pattern.

Study Limitations

We did not directly demonstrate that the earliest retrograde atrial activation sites within the CS were involved in the reentrant circuit by introducing late atrial extrastimuli or entrainment pacing[12] from the proximal CS sites and analyzing the return cycles. Because the earliest retrograde activation site within the CS was not primarily targeted during SP ablation, the essential effect of the ablations within the CS was unclear. More intensive ablations at the right inferoseptal and the midseptal region might have eliminated AVNRTs with the eccentric CS activation pattern by transseptal heating to the leftward PNE. Because left atrial mapping was not performed in any patients with the eccentric CS activation pattern, there was a possibility that the SP connected to the left atrium, not to the CS musculature. If it were the case, among six patients

with successful elimination of the eccentric SP, the ablation at the proximal CS might have indirectly injured the left atrial end of the eccentric SP from the roof of the proximal CS. In the other two patients with unsuccessful elimination of eccentric retrograde SP, the atrial end of the SP might be located at the left atrial site distant from the ablation site at the roof of the CS. In two patients with the concentric CS activation pattern in whom the classical SP ablation failed, the atrial end of the retrograde SP was not determined. The success criteria for SP ablation employed in our study (the elimination of the retrograde SP conduction) might be more rigorous as compared to those in previous studies (noninducibility criteria),[12,16,18] and the latter might be potentially enough to achieve a clinical success. Temporary oral medication (verapamil) in four of our patients with unsuccessful SP ablation might be potentially unnecessary because the medication was discontinued without a subsequent clinical recurrence. Even with CS venography, localization of the CS ostium was technically hard in some patients due to its funnel-like morphology.[24] Hence, the measurement of the distance from the CS ostium to the earliest atrial activation site within the CS might be inaccurate in some patients. Radiofrequency ablation within the proximal CS carries a risk of coronary artery stenosis.[25] As coronary angiography was not performed after ablation within the CS, asymptomatic stenosis in the coronary arteries cannot be definitely ruled out from the potential complications. The role of the Marshall vein in the genesis of eccentric CS activation pattern[20] was not assessed because the earliest activation site was not compatible with the commonly accepted location of the Marshall vein.

Conclusions

In 75% of atypical AVNRTs with the eccentric CS activation, the SP ablations within the CS were required to eliminate retrograde SP conductions and render AVNRTs noninducible, suggesting these retrograde SPs had left-sided breakthroughs and constituted the retrograde limbs of the reentry circuits. The mechanism of the eccentric CS activation pattern during atypical AVNRT might be due to the participation of the leftward PNE as a retrograde limb of the reentrant circuit.

References

1. Tawara S: Das Reitzleitungssystem des Säugetierherzens: Eine anatomischhistologische Studie über das Atrioventrikularbündel und die Purkinjeschen Fäden. Jena, Germany: Gustav Fischer, 1906, pp.135-136.
2. Inoue S, Becker AE: Posterior extensions of the human compact atrioventricular node: A neglected anatomic feature of potential clinical significance. Circulation 1998;97:188-193.
3. Anderson RH, Becker AE, Brechenmacher C, Davies MJ, Rossi L: The human atrioventricular junctional area. A morphological study of the A-V node and bundle. Eur J Cardiol 1975;3:11-25.
4. Inoue S, Becker AE, Riccardi R, Gaita F: Interruption of the inferior extension of the compact atrioventricular node underlies successful radio frequency ablation of atrioventricular nodal reentrant tachycardia. J Interv Card Electrophysiol 1999;3:273-277.
5. Medkour D, Becker AE, Khalife K, Billette J: Anatomic and functional characteristics of a slow posterior AV nodal pathway: Role in dual-pathway physiology and reentry. Circulation 1998;98:164-174.
6. Khalife K, Billette J, Medkour D, Martel K, Tremblay M, Wang J, Lin LJ: Role of the compact node and its posterior extension in normal atrioventricular nodal conduction, refractory, and dual pathway properties. J Cardiovasc Electrophysiol 1999;10:1439-1451.
7. Jackman WM, Beckman KJ, McClelland JH, Xunzhang W, Friday KJ, Roman CA, Moulton KP, Twidale N, Hazlitt HA, Prior MI, Oren J, Overholt ED, Lazzara R: Treatment of supraventricular tachycardia due to atrioventricular nodal reentry by radiofrequency catheter ablation of slow pathway conduction. N Engl J Med 1992;327:313-318.
8. Kilic A, Amasyali B, Kose S, Aytemir K, Celik T, Kursaklioglu H, Iyisoy A, Ozmen N, Yuksel C, Lenk MK, Isik E: Atrioventricular nodal reentrant tachycardia ablated from left atrial septum. Int Heart J 2005;46:1023-1031.
9. Sorbera C, Cohen M, Woolf P, Kalapatapu SR: Atrioventricular nodal reentry tachycardia: Slow pathway ablation using the transseptal approach. Pacing Clin Electrophysiol 2000;23:1343-1349.
10. Jais P, Haissaguerre M, Shah DC, Coste P, Takahashi A, Barold SS, Clementy J: Successful radiofrequency ablation of a slow atrioventricular nodal pathway on the left posterior atrial septum. Pacing Clin Electrophysiol 1999;22:525-527.
11. Altemose GT, Scott LR, Miller JM: Atrioventricular nodal reentrant tachycardia requiring ablation on the mitral annulus. J Cardiovasc Electrophysiol 2000;11:1281-1284.
12. Nam GB, Rhee KS, Kim J, Choi KJ, Kim YH: Left atrionodal connections in typical and atypical atrioventricular nodal reentrant tachycardias: Activation sequence in the coronary sinus and results of radiofrequency catheter ablation. J Cardiovasc Electrophysiol 2006;17:171-177.
13. Vijayaraman P, Kok LC, Rhee B, Ellenbogen KA: Unusual variant of atrioventricular nodal reentrant tachycardia. Heart Rhythm 2005;2:100-102.
14. Lockwood D, Otomo K, Wang Z, Forresti S, Nakagawa H, Beckman K, Scherlag BJ, Patterson E, Lazzara R, Jackman WM: Electrophysiologic characteristics of atrioventricular nodal reentrant tachycardia: Implications for the reentrant circuits In: Zipes DP, Jalife J, eds. *Cardiac Electrophysiology. From Cell to Bedside*. Fourth Edition. Philadelphia, PA: W.B. Saunders, 2004, pp. 537-557.
15. Heidbuchel H, Jackman WM: Catheter ablation of atypical atrioventricular nodal reentrant tachycardia. In: Zipes DP, Haissaguerre M, eds. *Catheter Ablation of Arrhythmias*. Second Edition. Armonk, NY: Futura Publishing Co., 2002, pp. 249-276.
16. Hwang C, Martin DJ, Goodman JS, Gang ES, Mandel WJ, Swerdlow CD, Peter CT, Chen PS: Atypical atrioventricular node reciprocating tachycardia masquerading as tachycardia using a left-sided accessory pathway. J Am Coll Cardiol 1997;30:218-225.
17. Sakabe K, Wakatsuki T, Fujinaga H, Oishi Y, Ikata J, Toyoshima T, Hiura N, Nishikado A, Oki T, Ito S: Patient with atrioventricular node reentrant tachycardia with eccentric retrograde left-sided activation: Treatment with radiofrequency catheter ablation. Jpn Heart J 2000;41:227-234.
18. Chen J, Anselme F, Smith TW, Zimetbaum P, Epstein LM, Papageorgiou P, Josephson ME: Standard right atrial ablation is effective for atrioventricular nodal reentry with earliest activation in the coronary sinus. J Cardiovasc Electrophysiol 2004;15:2-7.
19. Gupta N, Kangavari S, Peter CT, Chen PS: Mechanism of eccentric retrograde atrial activation sequence during atypical atrioventricular nodal reciprocating tachycardia. Heart Rhythm 2005;2:754-757.
20. Josephson ME: *Supraventricular Tachycardias. Clinical Cardiac Electrophysiology. Techniques and Interpretations*. Third Edition. Philadelphia: Lippincott Williams & Wilkins, 2002, pp. 168-271.
21. Hirao K, Otomo K, Wang X, Beckman KJ, McClelland JH, Widman L, Gonzalez MD, Arruda M, Nakagawa H, Lazzara R, Jackman WM: Para-Hisian pacing. A new method for differentiating retrograde conduction over an accessory AV pathway from conduction over the AV node. Circulation 1996;94:1027-1035.
22. Knight BP, Zivin A, Souza J, Flemming M, Pelosi F, Goyal R, Man C, Strickberger SA, Morady F: A technique for the rapid diagnosis of atrial tachycardia in the electrophysiology laboratory. J Am Coll Cardiol 1999;33:775-781.
23. Heidbuchel H, Jackman WM: Characterization of subforms of AV nodal reentrant tachycardia. Europace 2004;6:316-329.
24. Hummel JD, Strickberger SA, Man KC, Daoud E, Niebauer M, Morady F: A quantitative fluoroscopic comparison of the coronary sinus ostium in patients with and without AV nodal reentrant tachycardia. J Cardiovasc Electrophysiol 1995;6:681-686.
25. Aoyama H, Nakagawa H, Pitha JV, Khammar GS, Chandrasekaran K, Matsudaira K, Yagi T, Yokoyama K, Lazzara R, Jackman WM: Comparison of cryothermia and radiofrequency current in safety and efficacy of catheter ablation within the canine coronary sinus close to the left circumflex coronary artery. J Cardiovasc Electrophysiol 2005;16:1218-1226.

Spatial Distribution of Repolarization and Depolarization Abnormalities Evaluated by Body Surface Potential Mapping in Patients with Brugada Syndrome

MIKI YOKOKAWA, M.D.,* HIROSHI TAKAKI, M.D.,† TAKASHI NODA, M.D., PH.D.,* KAZUHIRO SATOMI, M.D., PH.D.,* KAZUHIRO SUYAMA, M.D., PH.D.,* TAKASHI KURITA, M.D., PH.D.,* SHIRO KAMAKURA, M.D., PH.D.,* and WATARU SHIMIZU M.D., PH.D.*

From the *Division of Cardiology, Department of Internal Medicine, and †Department of Cardiovascular Dynamics, National Cardiovascular Center, Suita, Japan

Background: *Mutations in sodium channel gene, SCN5A, have been identified in Brugada syndrome, but it is still unclear as to how sodium channel dysfunction relates to arrhythmogenesis. We examined spatial distribution of both repolarization and depolarization abnormalities in patients with Brugada syndrome by using 87-leads body surface potential mapping (BSPM).*

Methods: *BSPM was recorded under baseline condition and after pharmacological interventions in 28 patients with Brugada syndrome (27 males, 49 ± 14 years). The ST-segment amplitude 20 ms after the end of QRS (ST20), QRS duration, and corrected recovery time (RTc) were measured in all 87-leads, and averaged among 6-leads (D–F, 5–6) reflecting right ventricular outflow tract (RVOT) potentials and the other 81-leads.*

Results: *The ST20 was elevated at baseline, normalized by isoproterenol, and augmented by pilsicainide in only the RVOT. The RTc was longer at baseline and increased by pilsicainide in only the RVOT. On the other hand, the QRS duration was slightly widened at baseline, further increased by pilsicainide, but not changed by isoproterenol in both leads.*

Conclusions: *The ST-segment elevation and the RTc prolongation were localized and modulated by agents only in the RVOT region, while the slight QRS widening at baseline and further increase by pilsicainide were observed homogeneously. Our data suggest that depolarization abnormalities are distributed homogeneously, whereas repolarization abnormalities are localized in the RVOT. (PACE 2006; 29:1112–1121)*

brugada syndrome, ST-segment, body surface potential mapping, repolarization, depolarization

Introduction

Brugada syndrome is characterized by an accentuated ST-segment elevation in the right precordial leads V1 through V3, reflecting potentials of the right ventricular outflow tract (RVOT) and generally associated with sudden cardiac death secondary to a rapid polymorphic ventricular tachycardia (PVT) or ventricular fibrillation (VF).[1–10] In Brugada syndrome, both repolarization and depolarization abnormalities have been reported.[11–14] Transmural electrical heterogeneity of repolarization across the wall of the RVOT is thought to cause ST-segment elevation in the leads V1-V3.[15,16] On the other hand, depolarization abnormalities including prolongation of the P wave, QRS duration, and PR interval are frequently observed in patients with Brugada syndrome.[12] Mutations in sodium channel gene, *SCN5A*, have been identified in Brugada syndrome, but it is still unclear as to how depolarization abnormalities by sodium channel dysfunction relate to arrhythmogenesis.[17,18]

In the present study, we examined the spatial distribution of both repolarization and depolarization abnormalities in patients with Brugada syndrome by using 87-leads body surface potential mapping (BSPM) under baseline condition and after pharmacological interventions.

Methods

Patients Population

The study population consisted of 28 patients with Brugada syndrome who were admitted to the National Cardiovascular Center, Suita, Japan, between 2000 and 2004 (27 men, aged 17–72 years; mean 49 ± 14). Brugada syndrome was diagnosed

Address for reprints: Wataru Shimizu, M.D., Ph.D., Division of Cardiology, Department of Internal Medicine, National Cardiovascular Center, 5-7-1 Fujishiro-dai, Suita, Osaka 565-8565, Japan. Fax: +81-6-6872-7486; e-mail: wshimizu@hsp.ncvc.go.jp

Received April 3, 2006; revised June 7, 2006; accepted June 21, 2006.

when a Type 1 coved-type ST-segment elevation (≥0.2 mV at J point) was observed in more than one of the right precordial leads (V1 to V3) in the presence or absence of a sodium channel blocker, and in conjunction with one of the following: (1) documented VF or PVT, (2) a family history of sudden cardiac death at age < 45 years, Type 1 electrocardiogram (ECG) in family members, (3) inducibility of VF or PVT with programmed electrical stimulation, and (4) a history of aborted cardiac arrest with or without documentation of VF, syncopal episodes of unknown origin, or nocturnal agonal respiration.

The clinical characteristics of the 28 patients are shown in Table I. Seventeen patients (61%) had Type 1 coved-type ST-segment elevation in the baseline standard 12-leads ECG, while the remaining 11 patients showed Type 1 ECG after intravenous injection of sodium channel blockers. VF was documented in 4 patients (14%), 13 patients (46%) had syncopal episodes only, and the remaining 11 patients were asymptomatic. Nine patients (32%) had a family history of sudden cardiac death. Twenty-four patients underwent programmed ventricular electrical stimulation during electrophysiological study, and VF was induced in 19 of the 24 patients (79%). A mutation in the *SCN5A* was identified in four patients (14%).

Body Surface Potential Mapping

Eighty-seven-leads BSPM was recorded using a VCM-3000 (Fukuda Denshi Co., Tokyo, Japan) (Fig. 1).[19,20] Eighty-seven-leads were arranged in a lattice-like pattern (13 × 7 matrix), except for four leads on the mid-axillary lines, which covered the entire thoracic surface; 59-leads were located on the anterior chest (Columns A–I) and 28-leads on the back (Columns J–M). These 87-unipolar electrograms with Wilson's central terminals as a reference, the standard 12-leads ECG, and Frank X, Y, Z scalar leads were recorded simultaneously. Row 6 of the BSPM was coincident with the level of the parasternal second intercostal space, whereas row 4 coincided with the mid-clavicular fifth intercostal space. Columns A and I of the BSPM were located on the right and left mid-axillary lines, whereas column E was on the mid-sternal line. Columns C and G corresponded to the right and left mid-clavicular lines. Therefore, leads V1 and V2 of the 12-leads ECG were located between D5 and E5, and between E5 and F5 of the BSPM leads. The six particular leads (D–F, 5–6) were defined as representative of the RVOT area based on the data of our previous study.[21] The ECG data were scanned with multiplexers and digitized using analog-to-digital converters with a sampling rate of 1,000 samples/second per channel. The digitized data were stored on a floppy disk and transferred to a personal computer with the analysis program developed by our institution.

Table I.

Clinical Characteristics of the 28 Patients with Brugada Syndrome

Male/Female	27/1
Age (years)	49 ± 14 (17–72)
Spontaneous Type 1 ECG	17 (61%)
Documented VF	4 (14%)
Syncopal episode of unknown origin	13 (46%)
Family history of SCD	9 (32%)
Induced VF during EPS	19/24 (79%)
Positive for *SCN5A* mutation	4 (14%)
ICD implantation	21 (75%)

Values are mean ± SD for age. Age represents the age at which diagnosis of Brugada syndrome was made.
ECG = electrocardiogram; EPS = electrophysiological study; ICD = implantable cardioverter-defibrillator; SCD = sudden cardiac death; VF = ventricular fibrillation.

Repolarization and Depolarization Parameters in ECGs

In the present study, three parameters were evaluated (Fig. 2). As the repolarization parameters, we measured the amplitude of ST-segment 20 ms after the end of QRS (ST20) and recovery time (RT) defined as the interval between QRS-onset and maximum dV/dt point of T wave. The RTc was corrected by Bazett's method ($RTc = RT/\sqrt{RR}$), as previously reported.[19] As the depolarization parameter, QRS duration was measured. Each parameter was measured semi-automatically in all 87-leads by the computer analysis program developed by our institution. We averaged these ECG parameters among 6-leads ECG (D–F, 5–6) in the upper precordial region reflecting the RVOT potentials and among the remaining 81-leads ECG reflecting potentials of other region (Fig. 1), and then compared data between the two regions.

Algorithm for Determination of the End of QRS

The end of QRS (QRS-end) is difficult to determine especially in the right precordial leads manifesting ST-segment elevation in Brugada patients. Figure 3 illustrates the algorithm for determination of the QRS-end in each BSPM ECG. With superimposed 87-leads ECG, we first determined the onset of QRS by detecting the earliest deflection, and then determined the QRS-end provisionally by visual inspection of all 87-leads (Fig. 3, upper panel). Thereafter, we computed the first derivative of QRS voltage (dV/dt) in each lead and its algebraic summation of the absolute value indicated by the area colored in black (Fig. 3, lower panel).

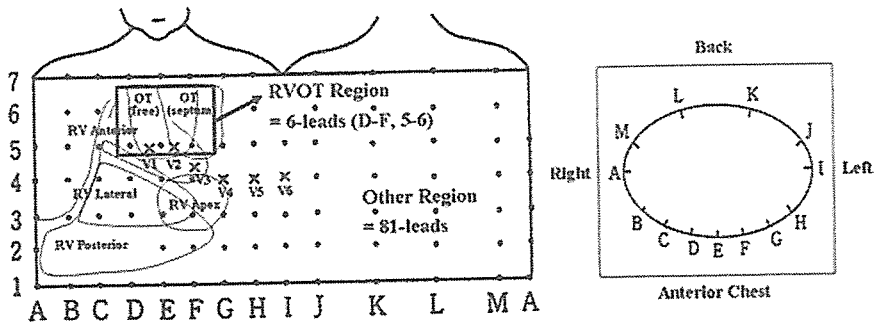

Figure 1. *Eighty-seven-leads body surface electrocardiogram (ECG). Plot of 87 unipolar electrode sites (•). Eighty-seven-leads points are arranged in a lattice-like pattern (13 × 7 matrix), except for 5 lead points on both mid-axillary lines, and covered the entire thoracic surface. The location of precordial 6 leads, V1–V6 in the 12-leads ECG is indicated by X. V1 and V2 leads of the ECG are located between D5 and E5, and between E5 and F5, respectively. The area of 6-leads ECG (D–F, 5–6) in the upper precordial area is defined as the RVOT region.*

The QRS-end was defined as the time-point where the cumulative area from the QRS-onset reached 98% of the total area.[22,23]

Pharmacological Interventions

After recording BSPM under baseline condition (Baseline-BSPM), isoproterenol, a β-adrenergic agonist, was infused at a constant rate of 0.02 $\mu gkg^{-1}min^{-1}$. When steady heart rate was achieved by isoproterenol infusion, BSPM was recorded (Isoproterenol-BSPM). After the effect of isoproterenol was completely washed out, pilsicainide, a class IC sodium channel blocker, was injected (5 mg every 1 minute) upto a maximum dose of 1 $mgkg^{-1}$ or 50 mg. BSPM was recorded 5 minutes after the completion of the drug, when the effect of the drug reached steady state (Pilsicainide-BSPM). Pilsicainide injection was stopped when Type 1 coved ST-segment elevation appeared or additional J-point elevation of $\geq$0.2 mV in case of baseline saddleback-type ST-segment was observed. Pilsicainide was also stopped when QRS duration was increased by $\geq$130% or spontaneous premature ventricular contractions were induced.

We compared the ECG parameters averaged among 6-leads of the RVOT region with those among 81-leads of the other region at baseline condition, after isoproterenol infusion, and pilsicainide injection.

Statistical Analysis

Numerical values were expressed as means ± SD, unless otherwise indicated. Comparisons of parameters before and after pharmacological interventions and those of each parameter between the 6-leads and 81-leads were made by using two-way repeated measures analysis of variance (ANOVA), followed by Scheffe's test. Comparisons of changes (Δ) in parameters with pharmacological interventions between the 6-leads and 81-leads were made

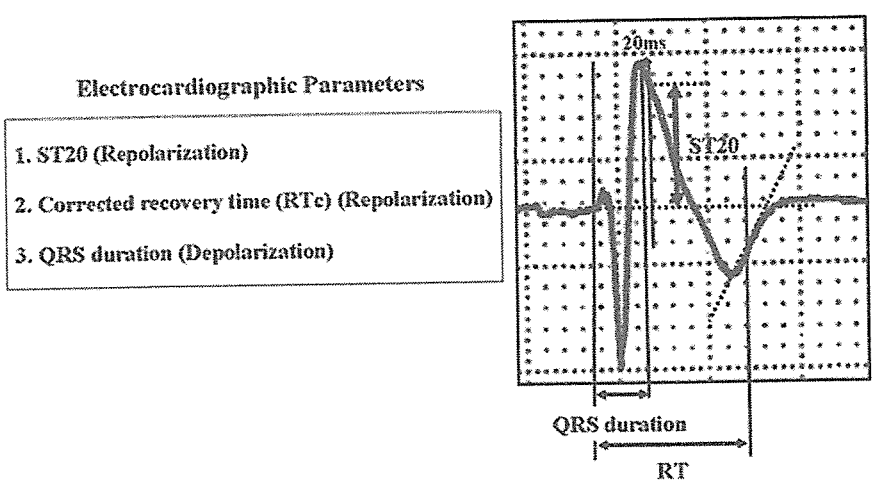

Figure 2. *Electrocardiographic parameters. As the repolarization parameters, the ST20 and corrected recovery time (RTc) were evaluated. The ST20 was defined as the amplitude of the ST-segment 20 ms after the end of QRS. The recovery time (RT) was defined as the interval between QRS-onset and maximum dV/dt point of T wave. As the depolarization parameter, the QRS duration was evaluated. Each parameter was measured semi-automatically in all 87-leads.*